WILEY | Hindawi

Research Article

Thermal Convective Instabilities and Chaos in a Rotating Hybrid Nanofluid Layer with Cattaneo–Christov Heat Flux Model

Sèmako Justin Dèdèwanou [1], **Adjimon Vincent Monwanou** [1],
Aimé Audran Koukpémèdji [1,2,3] **Amoussou Laurent Hinvi** [1,4]
Clément Hodévèwan Miwadinou [1,3,5] **and Jean Bio Chabi Orou** [1]

[1]*Laboratoire de la Mécanique des Fluides, de la Dynamique Non-Linéaire et de la Modélisation des Systèmes Biologiques (LMFDNMSB), Institut de Mathématiques et de Sciences Physiques (IMSP), Université d'Abomey-Calavi (UAC), Godomey, Benin*
[2]*Département de Physique, FAST-Natitingou, Université Nationale des Sciences, Technologies, Ingénierie et Mathématiques (UNSTIM) d'Abomey, Abomey, Benin*
[3]*Laboratoire de Physique et Applications du Centre Universitaire de Natitingou, Université Nationale des Sciences, Technologiques, Ingénierie et Mathématiques (UNSTIM) d'Abomey, Abomey, Benin*
[4]*Department of Industrial Computer and Electrical Engineering, Université Nationale des Sciences, Technologiques, Ingénierie et Mathématiques (UNSTIM) d'Abomey, Abomey, Benin*
[5]*Département de Physique, ENS-Natitingou, Université Nationale des Sciences, Technologies, Ingénierie et Mathématiques (UNSTIM) d'Abomey, Abomey, Benin*

Correspondence should be addressed to Aimé Audran Koukpémèdji; kaudranus2000@gmail.com

The linear and nonlinear dynamics of thermal convection of a rotating hybrid nanofluid layer heated from below with the Cattaneo–Christov heat flux model are studied in this paper. Starting from the flow equations of a hybrid nanofluid and exploiting the free boundary conditions, the analytical expressions of the stationary and oscillatory Rayleigh numbers of the base fluid are determined as a function of the dimensionless parameters of the heat transfer fluid and the thermophysical properties of the hybrid nanofluid. The effects of hybrid nanoparticles and Taylor number on the onset of stationary convection in the base fluid are investigated graphically. Then, a numerical study of the transition from natural convection to chaotic behaviour of the hybrid nanofluid is made using the truncated Galerkin approximation. This approximation allowed us to find a novel six-dimensional nonlinear system depending on the parameters of the base fluid and the thermophysical properties of the hybrid nanofluid that can be reduced to five, four, or three dimensions when we tend some parameters to zero. The different results showed that the addition of hybrid nanoparticles (alumina-copper) to a thermal fluid (water) subjected to the rotation force in the presence or absence of the thermal relaxation time allows control of the chaotic convection in the base fluid. On the other hand, the increase of the rescaled Taylor number and the Cattaneo number widens the domain of chaos in the hybrid nanofluid with the increase of the rescaled Rayleigh number of the base fluid.

1. Introduction

In 1995, Choi introduced, at the Argonne National Laboratory of the University of Chicago in the U.S., the concept of nanofluid [1]. This new generation of fluids consists of dispersing nanoparticles (assemblies of a few hundred to a few thousand atoms, leading to an object with at least one dimension of thousands of atoms, leading to an object of which at least one of the dimensions is of nanometric size) in a base liquid (water, oil, ethylene glycol, toluene). The use of

these nanofluids in some industrial operations that involve heat transfer by convection is a promising alternative solution to improve thermal performance. Thus, the problem of natural convection in a nanofluid layer heated from below has been studied by several researchers [2–6] with the Fourier law. The flow and heat transport of nanomaterial with quadratic radiative heat flux and aggregation kinematics of nanoparticles reported by Mahanthesh [7] revealed that the suspension of the nanoparticles increases the thermal conductivity and, thus, improves the temperature and reduces the heat flux at the plate. The Rayleigh-Bénard convection in nanofluid submerged with dust particles was investigated by Shalini and Mahanthesh [8]. They pointed out that the inclusion of nano and dust particles reduces the Rayleigh number while the rotation postpones the onset of convection and stabilizes the system.

Ahuja and Sharma [9] conducted a comprehensive review of the instability of Rayleigh-Bénard convection in nanofluids by summarizing in their work the studies related to the instability of a horizontal nanofluid layer under the impact of various parameters such as rotation magnetic field, Hall currents, and LTNE (local thermal nonequilibrium) effects in porous and nonporous media. The thermal convection in a rotating fluid layer provides a system to study hydrodynamic instabilities, pattern formation, and spatio-temporal chaos in nonlinear dynamical systems with many practical applications in engineering, such as food processing, chemical processes, solidification, centrifugal casting of metals, and rotating machines [10].

To compensate for the defect and all the disadvantages of mono nanofluids, it is essential to combine several nanoparticles to prepare a hybrid nanofluid [11]. Natural magnetohydrodynamic convection in a triangular cavity filled with a hybrid (copper-alumina)/water nanofluid with localized heating from below and internal heat has been investigated by Rashad et al. [12]. They concluded that a hybrid nanofluid composed of equal amounts of copper and alumina nanoparticles dispersed in water has no significant improvement on the average Nusselt number compared to the mono nanofluid and that the effect of increasing the hybrid nanoparticles becomes significant in the case where natural convection is very low. Aladin et al. [13] also studied the significant effects of suction and magnetic field on a moving plate containing a hybrid (copper-alumina)/water nanofluid. They have proved that the hybrid nanofluid gives better results than the mono nanofluid.

According to Myson and Mahanthesh [14], the hybrid nanofluid delays the convection and will further enhance the heat transfer rate, but the Casson parameter advances the convection while reducing the heat transfer rate. Mackolil and Mahanthesh [15] illustrated the optimization of heat transfer in the thermal Marangoni and nonlinear convective flow of a hybrid nanomaterial with sensitivity analysis. It is shown that the hybrid nanomaterial possesses enhanced thermal fields for nanoparticle volume fractions less than 0.02. The sensitivity computation of nonlinear convective heat transfer in hybrid nanomaterial between two concentric cylinders with irregular heat sources was also made by Thriveni and Mahanthesh [16].

Given its advantages and industrial applications, especially in chemical reactions, biological systems, crystal production, petroleum reservoir modeling, and packed-bed catalytic filtration, chaotic convection in a hybrid nanofluid layer should receive considerable attention due to the performance of nanofluids. Jawdat et al. [17], Moaddy et al. [18, 19], and Bhardwaj and Chawla [20] all contributed well to nonlinear dynamical analysis of the thermal convection in a horizontal nanofluid layer heated from below in the presence or absence of a magnetic field. They studied the effect of nanoparticles on chaotic convection in a layer of fluid (water) heated from below and noticed that the stability region can be increased by using nanofluids and that the onset of chaotic convection can be delayed under the influence of nanoparticles. Also, variations in temperature and magnetic field strength cause the system to transition from a steady state to chaos and back to a steady state. The case of hybrid nanofluid was first presented by Dèdèwanou et al. [21] with the Fourier law. They found that the copper nanofluid makes it possible to quickly switch from chaotic to periodic regimes compared to the alumina nanofluid, and the use of hybrid nanoparticles allows further control of the chaos in the base fluid by expanding the convective flow and reducing the chaotic flow.

Furthermore, Maxwell and Cattaneo modified Fourier's law by taking into account the aspect of thermal relaxation time in the propagation of heat [22]. In order to eliminate the heat flow and thus obtain a single equation for the temperature field, Christov [23] proposed a generalization of the material-invariant Maxwell–Cattaneo law, in which the relaxation time of the heat flow is given by the convex Oldroyd upper derivative. This new law was used by Straughan [24] to study thermal convection in an ordinary fluid. He concluded that the thermal relaxation time is significant if the Cattaneo number is large enough, and the convection mechanism changes from stationary to oscillatory convection with narrower cells. Indeed, some researchers used the Cattaneo–Christov model to appreciate the effects of temporal relaxation on the thermal behavior of a nanofluid [25–31]. Alebraheem and Ramzan [26] have studied the heat and mass transfer of Casson nanofluid flow containing gyrotactic microorganisms past a swirling cylinder by considering the Cattaneo-Christov heat flux model. According to their numerical solution of the subject system, which is framed via the bvp4c technique of MATLAB software, the concentration of the fluid is reduced owing to the increase in values of the brownian motion parameter and local Reynolds number, but the diminishing density of microorganisms is perceived for mounting estimates of the bioconvection Péclet number. Multiple slip impacts in the MHD hybrid nanofluid flow with Cattaneo–Christov heat flux and autocatalytic chemical reaction were investigated by Gul et al. [32]. They found that the fluid temperature is diminishing function of the thermal slips parameters but increased for high estimates of the heat source-sink and nanoparticle volume concentration parameters while entropy number augmented for higher thermal relaxation parameter and Reynolds number. Lu et al. [33] have also studied a thin film flow of nanofluid comprising carbon

nanotubes influenced by Cattaneo–Christov heat flux and entropy generation. They showed that the velocity and temperature distributions increase as the solid volume fraction escalates. Recently, a three-dimensional flow of gold-silver/engine oil hybrid nanofluid owing to a rotating disk of variable thickness with Cattaneo–Christov heat flux has been addressed by Zhang et al. [34]. They proved that the performance of the hybrid nanofluid is far better than the common nanofluid according to the surface temperature and heat transfer rate. This same remark is made from the results obtained for the model-based comparative study of magnetohydrodynamics unsteady hybrid nanofluid flow between two infinite parallel plates with particle shape effects [35]. Considering hybrid nanofluid Yamada-Ota and Xue flow models in a rotating channel with the modified Fourier law, it is observed that the velocity profile decreases for the higher rotation parameter while it increases for the escalated slip parameter, but the fluid concentration and temperature are on the decline for higher surface catalyzed reaction and thermal relaxation parameters respectively [36]. Ramdan et al. [37] have analyzed the hydrodynamic and heat characteristics of the three-dimensional flow of a steady, laminar, and incompressible convective graphene-copper oxide/water and graphene-silver/water hybrid nanofluids (used as a solar energy absorber) with varied particle shapes in a porous medium. Their study revealed that the rotational parameter has declined the velocity profiles but enhanced the temperature profiles, and the decline effect is significant in the case of graphene-copper oxide/water whereas the enhancement effect of temperature is significant for graphene-silver/water. A comparative analysis of magnetized partially ionized copper, copper oxide-water, and kerosene oil nanofluid flow with Cattaneo–Christov heat flux was made by Abid et al. [38]. They noted the greater effective thermal conductivity for copper-water partially ionized nanofluid as compared to other given partially ionized nanofluids (copper-kerosene oil, copper oxide-water/kerosene oil partially ionized nanofluids). Ramzan et al. [39] developed a mathematical model for the nanofluid flow containing carbon nanotubes with ethylene glycol as a base fluid in a rotating channel with an upper permeable wall by adding the Cattaneo–Christov heat flux's impact with thermal stratification. The displacement of the lower plate at variable velocity, caused by the rotation of the fluid, produces forced convection with rotation and centripetal impact. Nevertheless, the upper plate is porous. Chu et al. [40] investigated a numerical solution for MHD Maxwell nanofluid with gyrotactic microorganisms, a higher-order chemical reaction in the presence of variable source/sink, and Newtonian heating in a rotating flow on a deformable surface and noted that on incrementing the conjugate heat parameter and thermal relaxation time, the rate of heat transfer augments, but the rate of heat transfer decreases on varying the fluid relaxation time.

Despite all the above, the study of nanoparticles requires more attention due to their industrial uses. After inspecting the scientific literature, we noted that no work has yet addressed the chaotic aspect of thermal convection in hybrid nanofluids, taking into account the thermal relaxation time,

although this would be very useful in some applications like petroleum reservoir modeling, chemical reactions, thermal transport in biological tissue, and surgical operations. Nevertheless, Layek and Pati [41] studied the effects of thermal lag on the onset of convection, its bifurcations, and the chaos of a horizontal layer of the heated Boussinesq fluid underneath via a five-dimensional nonlinear system. A comparative study of the five-dimensional system obtained for the case of a hybrid nanofluid was made by Dèdèwanou et al. [42]. Therefore, the objective of the present paper is to investigate the effects of hybrid nanoparticles on the occurrence of thermal convection instability and chaos in a rotating fluid layer heated from below with the Cattaneo–Christov heat flux model. A specific objective is to determine the analytical expression for the stationary Rayleigh number that can be used to study the nonlinear dynamics of thermal convection in rotating hybrid nanofluid flow in the presence of thermal relaxation time. This work aims to study the different transition regimes as a function of the thermophysical properties of nanofluids and then to show the effects of hybrid nanoparticles, Taylor number, and Cattaneo number on the chaotic behavior of natural convection in a basic fluid such as water via dynamical systems.

In the next section, the thermal convection in an infinite horizontal rotating hybrid nanofluid layer with the hyperbolic Cattaneo–Christov heat flux is outlined. Section 3 discusses the theory of conduction, stationary convection, and oscillatory convection, where we generalize and simplify the expression for the Rayleigh number by deriving a number of new analytical results. In order to reduce the set of equations governing the dynamic behavior of thermal convection in the hybrid (alumina-copper)/water nanofluid, discretized models in four and six dimensions are developed in Section 4 using the Galerkin expansion. We have studied the nature of the nonlinear dynamics of the obtained dynamical systems and determined the fixed points by analyzing the stability of the stationary solutions. These analyses have allowed us to justify the influence of the hybrid alumina-copper nanoparticle, the Cattaneo number, and the Taylor number on number on the transition from chaos to periodicity and vice versa in the fluid. In Section 5, we present the different simulations performed, and the results obtained are discussed. The conclusions are drawn in Section 6.

2. Mathematical Modeling

2.1. Problem Formulation. We consider an infinite rectangular cavity with two horizontal walls maintained at different temperatures. This cavity, heated from below with a thermal relaxation time, is filled with a hybrid nanofluid (water and nanoparticles), subject to gravity acting downwards and to rotation. In order to develop our numerical model, it is necessary to adopt certain assumptions, namely, the flow is assumed to be permanent and incompressible, the mixture is assumed to be homogeneous, single-phase, Newtonian, the nanoparticles are spherical, and the mass transfer between the particles and the fluid is negligible. The Cartesian coordinate system used is such that the y-axis follows the

horizontal and the vertical z-axis is collinear with gravity. The geometry of our problem is presented in Figure 1.

2.2. Governing Equations.

In this section, we have studied the equations governing the dynamic and thermal fluxes with boundary conditions and nondimensional parameters characterizing the thermal convection in a rotating hybrid nanofluid layer in the presence of thermal relaxation time. Taking into account the listed assumptions and using the hybrid nanofluid model proposed in Section 3, the equations governing the conservation of mass, momentum, energy, and heat flux for a laminar flow of the hybrid nanofluid are written in their dimensional form respectively as follows [10, 42]:

$$\frac{\partial v_i}{\partial x_i} = 0, \tag{1}$$

$$\rho_{hf}\left[\frac{\partial v_i}{\partial t} + \left(v_j\frac{\partial v_i}{\partial x_j}\right)\right] = -\frac{\partial p}{\partial x_i} - \rho g e_i \\ + \mu_{hf}\nabla^2 v_i + 2\rho_{hf}\Omega_j\frac{\partial v_i}{\partial x_j}e_i, \tag{2}$$

$$(\rho Cp)_{hf}\left[\frac{\partial T}{\partial t} + \left(v_j\frac{\partial T}{\partial x_j}\right)\right] = -\frac{\partial Q_j}{\partial x_j}, \tag{3}$$

$$\left[\frac{\partial Q_i}{\partial t} + \left(v_j\frac{\partial Q_i}{\partial x_j}\right)\right] + Q_i = -k_{hf}\frac{\partial T}{\partial x_i}. \tag{4}$$

In equation (2), $e_i = (0, 0, 1)$ is the unit vector and $\nabla^2 = (\partial^2/\partial x^2) + (\partial^2/\partial y^2) + (\partial^2/\partial z^2)$ is the Laplacian operator. The use of the Boussinesq approximation allows us to define the density as a function of temperature as

$$\rho = \rho_{hnf}\left[1 - \beta_{hf}(T - T_0)\right]. \tag{5}$$

The density, thermal expansion coefficient, heat capacity, dynamic viscosity, thermal conductivity of the dynamic viscosity, and thermal conductivity of the hybrid nanofluid, respectively, are defined as follows:

$$\rho_{hf} = (1 - \varphi_2)\left[(1 - \varphi_1)\rho_f + \varphi_1\rho_{s1}\right] + \varphi_2\rho_{s2},$$

$$(\rho\beta)_{hf} = (1 - \varphi_2)\left[(1 - \varphi_1)(\rho\beta)_f + \varphi_1(\rho\beta)_{s1}\right] + \varphi_2(\rho\beta)_{s2},$$

$$(\rho Cp)_{hf} = (1 - \varphi_2)\left[(1 - \varphi_1)(\rho Cp)_f + \varphi_1(\rho Cp)_{s1}\right] + \varphi_2(\rho Cp)_{s2},$$

$$(\rho Cp)_{hf} = (1 - \varphi_2)\left[(1 - \varphi_1)(\rho Cp)_f + \varphi_1(\rho Cp)_{s1}\right] + \varphi_2(\rho Cp)_{s2},$$

$$\mu_f = \mu_{hf}(1 - \varphi_1)^{-2.5}(1 - \varphi_2)^{-2.5},$$

$$k_{hf} = k_{gf}\left[\frac{(k_{s2} + \eta k_{gf}) - \eta\varphi_2(k_{gf} - k_{s2})}{(k_{s2} + \eta k_{gf}) + \varphi_2(k_{gf} - k_{s2})}\right], \tag{6}$$
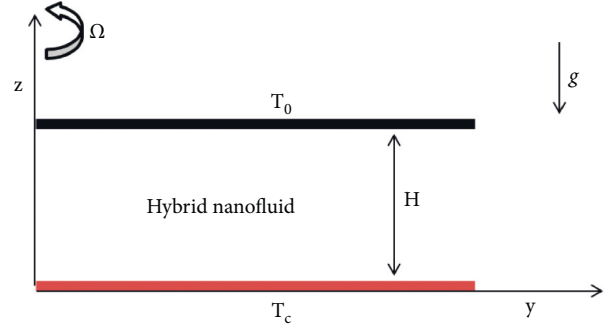
to

FIGURE 1: Configuration of the problem.

$$k_{hnf} = k_{hf}\left[\frac{(k_{s1} + \eta k_{hf}) - \eta\varphi_1(k_{hf} - k_{s1})}{(k_{s1} + \eta k_{hf}) + \varphi_1(k_{hf} - k_{s1})}\right], \tag{7}$$

where

$$\eta = m - 1. \tag{8}$$

The thermophysical properties of nanoparticles and water used in this work are summarized in Table 1 (see [13]).

3. Linear Stability Analysis

We consider a classical Rayleigh-Bénard problem of linear stability of convective rolls in a horizontal fluid layer with unconstrained boundary conditions. Thus, the temperature boundary conditions are $T = T_c$ at $z = 0$ and $T = T_0$ at $z = 1$ with $T_c > T_0$. As for the velocity, its component along the z axis is zero at the boundaries.

3.1. Steady-State Solutions.

A time-independent quiescent solution of equations (1)–(4) with temperature and heat flux varying in the z direction only, is obtained by reducing equations (2)–(4) to

$$\rho_{hf}\left(v_j\frac{\partial v_i}{\partial x_j}\right) + \frac{\partial p}{\partial x_i} + \rho g e_i - \mu_{hf}\nabla^2 v_i - 2\rho_{hf}\Omega_j\frac{\partial v_i}{\partial x_j}e_i = 0,$$

$$(\rho Cp)_{hf}\left(v_j\frac{\partial T}{\partial x_j}\right) + \frac{\partial Q_j}{\partial x_j} = 0, \quad (9)$$

$$\left(v_j\frac{\partial Q_i}{\partial x_j}\right) + Q_i + k_{hf}\frac{\partial T}{\partial x_i} = 0.$$

Then, the steady state solutions are given

$$\begin{aligned} v_b(z) &= 0, \\ T_b &= T_c - \chi x_j e_j, \\ Q_b(z) &= \chi k_{hf} \text{ and } P_b(z) = P_0, \end{aligned} \tag{10}$$

with the temperature gradient χ and the profile of P_0 defined by

TABLE 1: The thermophysical properties of the water and nanoparticles at 293 K.

	ρ	Cp	k	$\beta \times 10^{-5}$
Water	997.1	4179	0.613	21
Alumina	3970	765	40	0.85
Copper	8933	385	401	1.67

$$\chi = \left| \frac{\partial T}{\partial x_i} \right| \text{ and}$$

$$\frac{\partial p_0}{\partial x_i} = \rho(T_b) g e_i. \tag{11}$$

3.2. Simplified Set of Equations. In order to simplify the parametric representation of this physical problem and to find the characteristic properties of the system, it is necessary to recast the flow equations. Thus, the following normalized quantities are introduced:

$$\tilde{x}_i = \frac{x_i}{H},$$

$$\tilde{v}_i = \frac{\rho_f H . v_i}{\mu_f},$$

$$\tilde{P} = \frac{H^2 . P}{\rho_{f.} \nu_f},$$

$$t_* = \frac{\mu_f t}{\rho_{f.} H^2}, \tag{12}$$

$$\tilde{T} = \sqrt{\frac{\beta_f g k_f H^2}{\chi \nu_f (\rho Cp)_f}} T,$$

$$\tilde{Q}_i = \frac{H}{k_f} \left(\frac{\tilde{T}}{T} \right) Q_i.$$

Considering small perturbations on the basic solutions as follows:

$$\tilde{v}_i = \tilde{v}_b + \tilde{v}_i',$$
$$\tilde{T} = \tilde{T}_b + T',$$
$$\tilde{Q}_i = \tilde{Q}_b + Q_i', \tag{13}$$
$$\tilde{P} = \tilde{P}_b + \tilde{P}',$$

and neglecting the products of the primed quantities, we obtain the following dimensional equations:

$$\frac{\partial \tilde{v}_i'}{\partial \tilde{x}_i'} = 0, \tag{14}$$

$$\frac{\partial \tilde{v}_i'}{\partial \tilde{t}'} = -\frac{\partial \tilde{P}'}{\partial \tilde{x}_i'} + \left(\frac{\mu_{hf}}{\mu_f} \frac{\rho_f}{\rho_{hf}} \right) \nabla^2 \tilde{v}_i'$$
$$+ \frac{(\rho\beta)_{hf}}{(\rho\beta)_f} \sqrt{Ra_f} \tilde{T} e_i + \sqrt{Ta} \frac{\partial \tilde{v}_i'}{\partial \tilde{x}_j} e_i, \tag{15}$$

$$\left(\frac{(\rho Cp)_{hf}}{(\rho Cp)_f} \right) \left(Pr_f \frac{\partial \tilde{T}'}{\partial \tilde{t}'} - \sqrt{Ra_f} \tilde{w}' \right) = -\frac{\partial \tilde{Q}_i'}{\partial \tilde{x}_j}, \tag{16}$$

$$2Pr_f C_f \frac{\partial \tilde{Q}_i'}{\partial \tilde{t}'} + \tilde{Q}_i' = -\left(\frac{k_{hf}}{k_{hf}} \right) \frac{\partial \tilde{T}'}{\partial \tilde{x}_i'}, \tag{17}$$

where the dimensionless parameters are defined by

$$Pr_f = \frac{\mu_f}{\rho_f \alpha_f},$$

$$C_f = \frac{\alpha_f \tau}{2H^2}, \tag{18}$$

$$Ra_f = \frac{g . H^4 \beta_f \chi}{\alpha_f \nu_f}.$$

Now we eliminate the pressure from the nondimensional equations (14)–(17) by taking the curl-curl of equation (15), the divergence of equation (15), the inner product of any vector equation with e_i;, and denoting the divergence of the heat flux $Q = (\partial \tilde{Q}_i / \partial \tilde{x}_i)$, to obtain, after dropping the tilde notation for brevity, the equations

$$\frac{\partial}{\partial t} (\nabla^2 w) = \sqrt{Ra_f} \frac{(\rho\beta)_{hf}}{(\rho\beta)_f} \left(\frac{\partial^2 T}{\partial x^2} + \frac{\partial^2 T}{\partial y^2} \right)$$
$$+ \left(\frac{\mu_{hf}}{\mu_f} \frac{\rho_f}{\rho_{hf}} \right) \nabla^4 w + \sqrt{Ta} \frac{\partial \zeta}{\partial z}, \tag{19}$$

$$\left(\frac{(\rho Cp)_{hf}}{(\rho Cp)_f} \right) \left(Pr_f \frac{\partial T}{\partial t} - \sqrt{Ra_f} w \right) = -Q, \tag{20}$$

$$2Pr_f C_f \frac{\partial Q}{\partial \tilde{t}'} + Q = -\left(\frac{k_{hf}}{k_{hf}} \right) \nabla^2 T. \tag{21}$$

which describe the evolution of the conduction steady state perturbations in a conveniently simplified form with four variables such as the z-component of the velocity field, the vorticity $\zeta = \partial v / \partial x - \partial u / \partial y$, the heat flux Q, and the temperature T.

An evolutionary equation for the vorticity can be obtained from the equation of motion by taking curl, then the dot product with e_3 for the vertical component. Thus, eliminating the pressure and introducing the vorticity in equation (2) allows us to obtain the following:

$$\left[\left(\frac{\mu_{hf}}{\mu_f} \frac{\rho_f}{\rho_{hf}} \right) \nabla^2 - \frac{\partial}{\partial t} \right] \zeta = -\sqrt{Ta} \frac{\partial w}{\partial z}. \tag{22}$$

From equations (19) and (22), we obtain the following:

$$\left[\left(\left(\frac{\mu_{hf}}{\mu_f}\frac{\rho_f}{\rho_{hf}}\right)\nabla^2 - \frac{\partial}{\partial t}\right)\left(\frac{\partial}{\partial t}\nabla^2 - \left(\frac{\mu_{hf}}{\mu_f}\frac{\rho_f}{\rho_{hf}}\right)\nabla^4 + Ta\frac{\partial^2}{\partial z^2}\right)\right]w$$

$$-\sqrt{Ra_f}\,\frac{(\rho\beta)_{hf}}{(\rho\beta)_f}\left[\left(\frac{\mu_{hf}}{\mu_f}\frac{\rho_f}{\rho_{hf}}\right)\nabla^2 - \frac{\partial}{\partial t}\right]\left(\frac{\partial^2 T}{\partial x^2} + \frac{\partial^2 T}{\partial y^2}\right) = 0. \tag{23}$$

3.3. Normal Modes and Analytical Solution. The linear stability of the conduction solutions is studied by writing the perturbations in separable form and assuming an exponential time dependence

$$w = W(z)h(x, y)e^{\sigma t},$$
$$T = \Theta(z)h(x, y)e^{\sigma t}, \tag{24}$$
$$Q = \Phi(z)h(x, y)e^{\sigma t},$$

with the plane tiling function satisfying

$$\nabla^2 h(x, y) = -\kappa^2 h(x, y), \tag{25}$$

where W, Θ, Φ are eigenfunctions. The substitution of equation (24) into the differential equations (20), (21), and (23) leads to

$$\left[\left(D^2 - \kappa^2\right)\left(\gamma_1\left(D^2 - \kappa^2\right) - \sigma\right)^2 + TaD^2\right] \tag{26}$$
$$W = \kappa^2\gamma_2\sqrt{Ra_f}\left[\gamma_1\left(D^2 - \kappa^2\right) - \sigma\right]\Theta,$$

$$\sigma Pr_f\Theta = \sqrt{Ra_f}W - \gamma_3\Phi, \tag{27}$$

$$2\sigma Pr_f C_f\Phi + \Phi = -\gamma_4\left(D^2 - \kappa^2\right)\Theta, \tag{28}$$

where $D = d/dt, D^2 = d^2/dt^2$ and

$$\gamma_1 = \frac{\mu_{hf}}{\mu_f}\frac{\rho_f}{\rho_{hf}},$$

$$\gamma_2 = \frac{(\rho\beta)_{hf}}{(\rho\beta)_f},$$

$$\gamma_3 = \frac{(\rho Cp)_f}{(\rho Cp)_{hf}},$$

$$\gamma_4 = \frac{k_{hf}}{k_{hf}}. \tag{29}$$

Equations (26)–(28), which represent the starting point for analytical and numerical calculations on thermal convective instability are used to study the occurrence of stationary and oscillatory convection in nanofluids. They are equivalent to those obtained by Straughan [24] and Bissell [43, 44] in the case of an ordinary fluid not subjected to a Coriolis force, i.e. when $\varphi_1 = \varphi_2 = 0$ and $Ta = 0$. The disappearance of tangent shear stresses at the free surface and the conservation of the mass equation allow us to obtain the boundary conditions of the free surface defined by

$$W = 0,$$
$$D^2W = 0 \text{ and} \tag{30}$$
$$\Theta = 0 \text{ at } z = 0, 1.$$

In order to obtain an approximate solution of equations (26)–(28), we used the Galerkin weighted residual method by choosing the test function written as

$$W = W_0\sin(\pi z),$$
$$\Theta = \Theta_0\sin(\pi z), \tag{31}$$
$$\Phi = \Phi_0\sin(\pi z),$$

which fulfill the conditions at the borders mentioned in equation (30).

By substituting the test functions defined in equation (31) into equations (26)–(28) and performing some integrations, we obtain the following matrix equation:

$$\begin{pmatrix} \left[J(\gamma_1 J + \sigma) + \dfrac{\pi^2 Ta}{(\gamma_1 J + \sigma)}\right] & -\kappa^2\gamma_2\sqrt{Ra_f} & 0 \\[2ex] -\sqrt{Ra_f} & \sigma Pr_f & \gamma_3 \\[2ex] 0 & -\gamma_4 J & \left(2\sigma Pr_f C_f + 1\right) \end{pmatrix}$$

$$\times\begin{pmatrix} W_0 \\ \Theta_0 \\ \Phi_0 \end{pmatrix} = \begin{pmatrix} 0 \\ 0 \\ 0 \end{pmatrix}, \tag{32}$$

where $J = D^2 - \kappa^2$. For this matrix equation (32) to admit a nontrivial solution, the Rayleigh number of the base fluid must be in the following form:

$$Ra_f = \frac{\left[\gamma_3\gamma_4 J + \sigma Pr_f\left(2\sigma Pr_f C_f + 1\right)\right]\left[J(\gamma_1 J + \sigma) + \left(\pi^2 Ta/(\gamma_1 J + \sigma)\right)\right]}{\kappa^2\gamma_2\left(2\sigma Pr_f C_f + 1\right)}. \tag{33}$$

For the following, let $\sigma = j\omega$ with $j^2 = -1$ and ω the real frequency. Thus, the expression for the Rayleigh number defined in equation (33) becomes

$$Ra_f = \Delta_1 + j\omega\Delta_2, \tag{34}$$

with

$$\Delta_1 = \left[\kappa^2\gamma_2\left(1 + 4\omega^2 Pr_f^2 C_f^2\right)\right]^{-1}$$
$$\cdot \left[J\left(\gamma_1\gamma_3\gamma_4 J^2 - \omega^2 Pr_f\right) + \frac{\pi^2 Ta\left(\gamma_1\gamma_3\gamma_4 J^2 + \omega^2 Pr_f\right)}{\left(\gamma_1 J\right)^2 + \left(\omega\right)^2}\right.$$
$$\left. + 2J\omega^2 Pr_f C_f\left(\gamma_3\gamma_4 J - 2\omega^2 Pr_f^2 C_f\right) + \frac{2\pi^2\omega^2 Pr_f C_f Ta\left(2\omega^2 Pr_f^2 C_f - \gamma_3\gamma_4 J\right)}{\left(\gamma_1 J\right)^2 + \left(\omega\right)^2}\right], \tag{35}$$

$$\Delta_2 = \left[\kappa^2\gamma_2\left(1 + 4\omega^2 Pr_f^2 C_f^2\right)\right]^{-1}$$
$$\cdot \left[J^2\left(\gamma_3\gamma_4 + \gamma_1 J\right) + \frac{\pi^2 JTa\left(\gamma_1 - \gamma_3\gamma_4\right)}{\left(\gamma_1 J\right)^2 + \left(\omega\right)^2} + 2JPr_f C_f\left(2\gamma_1 J\omega^2 Pr_f^2 C_f - \gamma_1\gamma_3\gamma_4 J^2\right) + \frac{2\pi^2\gamma_1 JPr_f C_f Ta\left(2\omega^2 Pr_f^2 C_f - \gamma_3\gamma_4 J\right)}{\left(\gamma_1 J\right)^2 + \left(\omega\right)^2}\right]. \tag{36}$$

Since the Rayleigh number is a real and positive physical quantity, then for the expression equation (33) to exist, ω must be zero or $\Delta_2 = 0$.

3.4. Stationary Convection.
According to the stability exchange principle for the stationary case, the stability margin is characterized by the frequency equal to zero. This condition allows to obtain from the expression equation (33), the Rayleigh number of the base fluid of the stationary convection expressed as follows:

$$Ra_f^{st} = \frac{\gamma_3\gamma_4}{\kappa^2\gamma_2}\left[\gamma_1\left(\kappa^2 + \pi^2\right)^3 + \frac{\pi^2 Ta}{\gamma_1}\right]. \tag{37}$$

If $\gamma_1 = \gamma_2 = \gamma_3 = \gamma_4 = 1$ and the cavity is not rotating, i.e. $\varphi_1 = \varphi_2 = 0$ and $Ta = 0$, equation (37) is equivalent to the classical Rayleigh number of stationary convection in ordinary fluids [42].

In the absence of the rotation force, we have

$$Ra_f^{st} = \frac{\gamma_1\gamma_3\gamma_4}{\gamma_2}\frac{\left(\kappa^2 + \pi^2\right)^3}{\kappa^2}. \tag{38}$$

The absolute critical Rayleigh number of the hybrid nanofluid in this case is defined as

$$Ra_f^{st} = \frac{27\pi^4}{4}\frac{\gamma_1\gamma_3\gamma_4}{\gamma_2}, \tag{39}$$

with the corresponding wavenumber

$$\kappa_c^{st} = \frac{\pi}{\sqrt{2}}. \tag{40}$$

We note that the Rayleigh number obtained for stationary convection in nanofluids is not a function of the Prandtl number or the Cattaneo number of the base fluid. Thus, the same results can be associated with the more usual Fourier law for mono nanofluids or hybrid nanofluids.

3.5. Oscillatory Convection.
Now, we study the effects of the Cattaneo number, the nanoparticles, and the rotation on the oscillating convection. In this case, we must have $\omega \neq 0$ and $\Delta_2 = 0$. Therefore, the Rayleigh number of the base fluid for oscillatory convection is given by

$$Ra_f^{os} = \left[\kappa^2\gamma_2\left(1 + 4\omega^2 Pr_f^2 C_f^2\right)\right]^{-1}$$
$$\cdot \left[J\left(\gamma_1\gamma_3\gamma_4 J^2 - \omega^2 Pr_f\right) + \frac{\pi^2 Ta\left(\gamma_1\gamma_3\gamma_4 J^2 + \omega^2 Pr_f\right)}{\left(\gamma_1 J\right)^2 + \left(\omega\right)^2}\right.$$
$$+ 2J\omega^2 Pr_f C_f\left(\gamma_3\gamma_4 J - 2\omega^2 Pr_f^2 C_f\right)$$
$$\left. + \frac{2\pi^2\omega^2 Pr_f C_f Ta\left(2\omega^2 Pr_f^2 C_f - \gamma_3\gamma_4 J\right)}{\left(\gamma_1 J\right)^2 + \left(\omega\right)^2}\right]. \tag{41}$$

The corresponding oscillatory frequency ω must verify the following equations:

$$\left(4\gamma_1 J^2 Pr_f^3 C_f^2\right)\omega^4 + \left[J^2\left(\gamma_3\gamma_4 + \gamma_1 Pr_f\right)\right.$$
$$+ 4\gamma_1 JPr_f^3 C_f^2\left(\gamma_1 J^3 + \pi^2 Ta\right) - 2\gamma_1\gamma_3\gamma_4 Pr_f C_f J^3\right]\omega^2$$
$$+ \left[\gamma_1^2 J\left(\gamma_3\gamma_4 + \gamma_1 Pr_f\right) + \pi^2 JTa\left(\gamma_1 - \gamma_3\gamma_4\right)\right. \tag{42}$$
$$\left. - 2\gamma_1\gamma_3\gamma_4 Pr_f C_f J^2\left(\gamma_3\gamma_4 + \gamma_1 Pr_f\right)\right] = 0.$$

For oscillatory instability to be possible, the value of ω^2 generated by equation (42) must be positive.

4. Dynamical System Analysis

In order to explore how thermal relaxation time, hybrid nanoparticles, and rotation affect the nonlinear stability of the onset of thermal convection in a horizontal layer of ordinary fluid such as water, we reduce the problem to the classical case of two-dimensional convective rolls in a fluid layer with unconstrained horizontal boundaries. Thus, we

assume that all physical quantities are independent of x. We consider the early stages of nonlinear convection when the basic structure of the convective rolls is still determined by the dynamic behavior of the linearized solution. The real components of the fluid velocity are expressed in terms of partial derivatives of the stream function as follows:

$$u = -\frac{\partial\psi(y,z,t)}{\partial z},$$
$$w = \frac{\partial\psi(y,z,t)}{\partial y}. \tag{43}$$

Eliminating the pressure from equation (2) and introducing the expressions of the stream function defined in equations (43) into the resulting equation and equations (3) and (4), we obtain with the appropriate dimensionless variables [10, 42], the following new equations:

$$\left[\left(\frac{1}{Pr_f}\frac{\partial}{\partial t_*} - \gamma_5\nabla^2\right)^2 - Ta\frac{\partial^2}{\partial z_*^2}\right]\frac{\partial^2\psi_*}{\partial y_*^2} = \gamma_6 Ra_f\left(\frac{1}{Pr_f}\frac{\partial}{\partial t_*} - \gamma_5\nabla^2\right)\frac{\partial^2 T_*}{\partial y_*^2}, \tag{44}$$

$$\left(1 + 2C_f\frac{d}{dt_*}\right)\left(\frac{dT_*}{dt_*} - \frac{\partial\psi_*}{\partial y_*}\right) = \gamma_7\left(\frac{\partial^2 T_*}{\partial y_*^2} + \frac{\partial^2 T_*}{\partial z_*^2}\right), \tag{45}$$

with

$$\frac{d}{dt_*} = \frac{\partial}{\partial t_*} - \frac{\partial\psi_*}{\partial z_*}\frac{\partial}{\partial y_*} + \frac{\partial\psi_*}{\partial y_*}\frac{\partial}{\partial z_*},$$

$$Ra_f = \frac{g.H^3\beta_f\left(T_c - T_0\right)}{\alpha_f\nu_f},$$

$$Pr_f = \frac{\nu_f}{\alpha_f},$$

$$C_f = \frac{\tau\alpha_f}{2H^2}, \tag{46}$$

$$\gamma_5 = \frac{\mu_{hf}}{\mu_f}\frac{\rho_f}{\rho_{hf}}\frac{k_f}{k_{hf}}\frac{(\rho Cp)_{hf}}{(\rho Cp)_f},$$

$$\gamma_6 = \frac{(\rho\beta)_{hf}}{(\rho\beta)_f}\frac{\rho_{hf}}{\rho_{hf}},$$

$$\gamma_7 = \frac{k_{hf}}{k_f}\frac{(\rho Cp)_f}{(\rho Cp)_{hf}}.$$

The ratio of the Rayleigh number of the hybrid nanofluid to that of the base fluid gives the effective Rayleigh number of the hybrid nanofluid as a function of the thermophysical properties and Rayleigh number of the heat transfer fluid defined as

$$Ra_f = \left(\frac{(\rho\beta)_{hf}}{(\rho\beta)_f}\right)\left(\frac{k_f}{k_{hf}}\right)\left(\frac{(\rho Cp)_{hf}}{(\rho Cp)_f}\right)\left(\frac{\mu_f}{\mu_{hf}}\right)Ra_f. \tag{47}$$

Similarly, the Cattaneo number of the hybrid nanofluid is defined as follows:

$$C_{hf} = \gamma_7 C_f. \tag{48}$$

4.1. Reduced Set of Equations. The solution of the coupled nonlinear system of partial differential equations (44) and (45) will be obtained by representing the current function and the temperature using the Galerkin expansion in the following form [42]:

$$\psi_*\left(y_* z_* t_*\right) = A_{11}\left(t_*\right)\sin\left(\kappa y_*\right)\sin\left(\pi z_*\right),$$
$$T_*\left(y_* z_* t_*\right) = B_{11}\left(t_*\right)\cos\left(\kappa y_*\right)\sin\left(\pi z_*\right) \tag{49}$$
$$+ B_{02}\left(t_*\right)\sin\left(\pi z_*\right).$$

This representation is equivalent to a Galerkin expansion of the solution in the y and z directions, truncated when $i + j = 2$, where i is the Galerkin summation index in the y direction and j is the Galerkin summation index in the z direction. Substituting equations (49) into equations (44) and (45), multiplying the equations by the orthogonal eigenfunctions corresponding to equations (44), and integrating over the domain and wavelength of the convection cell in the vertical and horizontal directions respectively, i.e., $\int_0^{\pi/\kappa} dy \int_0^1 dz\,(.)$, we obtain a set of three ordinary differential

equations for the time evolution of the second-order amplitudes expressed by

$$\frac{d^2 A_{11}}{dt_*^2} = -2\gamma_5 Pr_f\left(\kappa^2 + \pi^2\right)\frac{dA_{11}}{dt_*} - \gamma_5^2 Pr_f^2\left(\kappa^2 + \pi^2\right)^2 A_{11} - \pi^2 Pr_f^2 Ta A_{11} + \frac{\gamma_6\kappa^2 Pr_f Ra_f}{\left(\kappa^2 + \pi^2\right)}A_{11} + \gamma_6\kappa^2 Pr_f Ra_f\left(\gamma_5 Pr_f - \gamma_7\right),$$

$$\frac{d^2 B_{02}}{dt_*^2} = \frac{1}{2C_f}\left[\frac{dB_{02}}{dt_*} + \frac{\pi\kappa}{2}A_{11}B_{11} - 4\pi^2\gamma_7 B_{02}\right] - \frac{\pi\kappa^2}{2}A_{11}^2 + \frac{\pi\kappa}{2}\left(A_{11}\frac{dB_{11}}{dt_*} + B_{11}\frac{dA_{11}}{dt_*}\right) + \pi^2\kappa^2 A_{11}^2 B_{11} + \pi\kappa A_{11}\frac{dB_{11}}{dt_*},$$ (50)

$$\frac{d^2 B_{02}}{dt_*^2} = \frac{1}{2C_f}\left[\frac{dB_{02}}{dt_*} + \frac{\pi\kappa}{2}A_{11}B_{11} - 4\pi^2\gamma_7 B_{02}\right] - \frac{\pi\kappa^2}{2}A_{11}^2 + \frac{\pi\kappa}{2}\left(A_{11}\frac{dB_{11}}{dt_*} + B_{11}\frac{dA_{11}}{dt_*}\right) + \pi^2\kappa^2 A_{11}^2 B_{11} + \pi\kappa A_{11}\frac{dB_{11}}{dt_*}.$$

After introducing new variables of amplitudes defined as

$$U = \frac{(\kappa/\kappa_c)A_{11}}{(\kappa/\kappa_c)^2 + 2},$$

$$Y = \kappa R_f B_{11},$$ (51)

$$Z = \pi R_f B_{02},$$

and the expressions

$$R_f = \frac{Ra_f}{Ra_{fc}},$$

$$t_* = \left(\kappa^2 + \pi^2\right)t,$$

$$\lambda = \frac{8}{\left[(\kappa/\kappa_c)^2 + 2\right]},$$

$$Ra_{fc} = \frac{\epsilon\left(\kappa^2 + \pi^2\right)^3}{\kappa^2},$$

$$\delta = \frac{1}{2C_f\left(\kappa^2 + \pi^2\right)},$$

$$T_f = \frac{\pi^2 Ta}{\left(\kappa^2 + \pi^2\right)^3},$$

$$\epsilon = \frac{(\rho\beta)_f}{(\rho\beta)_{hf}}\frac{\alpha_{hf}}{\alpha_f}\frac{\mu_{hf}}{\mu_f},$$

$$\kappa_c = \frac{\pi}{\sqrt{2}},$$ (52)

in equations 50, we obtain the following system:

$$\begin{cases} \ddot{U} = -2\gamma_5 Pr_f\dot{U} + Pr_f\left[\gamma_6\epsilon R_f - Pr_f\left(T_f + \gamma_5^2\right)\right]U - \gamma_6 Pr_f\left[UZ - \left(\gamma_5 Pr_f - \gamma_7\right)\right]Y, \\ \ddot{Y} = \epsilon R_f\dot{U} + U^2 Y - 2U\dot{Z} - \dot{U}Z + \delta\left(\epsilon R_f U - \dot{Y} - UZ - \gamma_7 Y\right), \\ \ddot{Z} = \dot{U}Y + 2U\dot{Y} - \epsilon R_f U^2 + U^2 Z + \delta\left(UY - \dot{Y} - \lambda\gamma_7 Z\right). \end{cases}$$ (53)

Therefore, we can reduce the amplitude equations of system (53) to a system of first-order nonlinear equations by introducing the amplitudes $V = \dot{U}$, $P = \epsilon R_f U - \dot{Y} - UZ$, and $S = UY - \dot{Z}$. Thus, we obtain the six-dimensional system

by describing the nonlinear dynamic behavior of thermal convection in mono or hybrid nanofluids, presented as follows:

$$\begin{cases} \dot{U} = V, \\ \dot{Y} = \epsilon R_f U - P - UZ, \\ \dot{Z} = UY - S, \\ \dot{P} = US - \delta\left(P - \gamma_7 Y\right), \\ \dot{S} = UP - \delta\left(S - \lambda\gamma_7 Z\right), \\ \dot{V} = -2\gamma_5 Pr_f V + Pr_f\left[\gamma_6\epsilon R_f - Pr_f\left(T_f + \gamma_5^2\right)\right]U - \gamma_6 Pr_f\left[UZ - \left(\gamma_5 Pr_f - \gamma_7\right)\right]Y, \end{cases}$$ (54)

where the dot (.) denote the time derivative d/dt.

When $\varphi_1 = \varphi_2 = 0$, $\varphi_1 \neq 0$ and $\varphi_2 = 0$, $\varphi_1 = 0$ and $\varphi_2 = 0$, system equation (63) corresponds to the base fluid, alumina-water nanofluid, copper-water nanofluid, respectively.

When $T_f = 0$, system (63) is equivalent to the system obtained by Dèdèwanou et al. [42]. When $\varphi_1 = \varphi_2 = 0$,

$$\begin{cases} \dot{U} = V, \\ \dot{Y} = \epsilon R_f U - \gamma_7 Y - UZ, \\ \dot{Z} = UY - \lambda\gamma_7 Z, \\ \dot{V} = -2\gamma_5 Pr_f V + Pr_f\left[\gamma_6 \epsilon R_f - Pr_f\left(T_f + \gamma_5^2\right)\right]U - \gamma_6 Pr_f\left[UZ - \left(\gamma_5 Pr_f - \gamma_7\right)\right]Y. \end{cases} \tag{55}$$

Lorenz [45] has investigated the nonlinear analysis of convection in pure fluid confined in a nonporous cavity by using the Fourier law. His nonlinear dynamic system has been analyzed and solved for $Pr_f = 10$, so that there are convection cells in the domain and that the boundary conditions are satisfied [45, 46]. Bissell [43] analyzed the oscillatory convection with the Cattaneo–Christov hyperbolic heat-flow model and included the effects owing to Prandtl number, which in some circumstances can be used as a control parameter. He showed that the Cattaneo threshold can be conceived equivalently as a Prandtl threshold, so that system bifurcations could potentially be triggered by varying the Prandtl number. For small values of Cattaneo number, a five-dimensional nonlinear system obtained by Layek and Pati [41] undergoes a subcritical transition to chaos similar to the Lorenz system but undergoes a period-doubling transition to chaos when $Pr_f = 5$ and $C_f = 0.001$. For increasing values of Prandtl number, he found that the fine-structure of the period-doubling cascade is interrupted and that this is due to the generation of internal noise that fastens the transitional process. With the critical value of the wavenumber corresponding to the convection threshold, the expression of the Rayleigh number of the base fluid defined in equation (53) gives: $Ra_{fc} = 27\pi^4\epsilon/4$.

4.2. Dissipation Effect. The nonlinear dynamical system (54) has the reflection symmetry $(U, Y, P) \longrightarrow -(U, Y, P)$ and

$$\vec{\nabla}.\vec{\vartheta} = \frac{\partial\dot{U}}{\partial U} + \frac{\partial\dot{Y}}{\partial Y} + \frac{\partial\dot{Z}}{\partial Z} + \frac{\partial\dot{P}}{\partial P} + \frac{\partial\dot{S}}{\partial S} + \frac{\partial\dot{V}}{\partial V}, \tag{56}$$

$$\vec{\nabla}.\vec{\vartheta} = -\left[Pr_f\left(2\gamma_5 + \gamma_6\right) + 2\delta\right].$$

We note that $\vec{\nabla}.\vec{\vartheta} < 0$ whatever the values of Pr_f, γ_5, γ_6 and δ. Then system (54) is dissipative and its solutions are bounded in phase space. Therefore, if a set of initial points in phase space occupies the region $\vartheta(0)$ at $t = 0$, then after

$C_f = 0$, system (54) is equivalent to the system obtained by Gupta et al. [10].

When $\varphi_1 = \varphi_2 = 0$, $T_f = 0$, system (54) is equivalent to the system obtained by Layek and Pati [41].

In the absence of the thermal relaxation time, (54) and (46) are reduced to the following system:

some time, t, the end points of the corresponding trajectories will fill a volume

$$\vartheta(t) = \exp\left\{-\left[Pr_f\left(2\gamma_5 + \gamma_6\right) + 2\delta\right]t\right\}. \tag{57}$$

4.3. Equilibrium Points and Their Stability. In this section, the nature of the nonlinear dynamics of systems (54) and (55) is determined around the fixed points by analyzing the stability of stationary solutions. The hybrid nanofluid is confined in a nonporous cavity so that there are convection cells in the domain and the boundary conditions are satisfied.

4.3.1. The Case of $C_f = 0$. Considering the general form of system (54) defined by $\dot{X} = F(X_s)$ and the equilibrium (stationary or fixed) points X_s defined by $F(X_s) = 0$, we obtained three fixed equilibrium points of the system, including the first one

$$U_1 = Y_1 = Z_1 = P_1 = S_1 = V_1 = 0, \tag{58}$$

is the stationary solution and the other two

$$U_{2,3} = \pm\sqrt{\frac{-\lambda\gamma_5\gamma_6\gamma_7}{\left(T_f + \gamma_5^2\right)}\left[\frac{\gamma_7}{\gamma_5\gamma_6}\left(T_f + \gamma_5^2\right) - \epsilon R_f\right]},$$

$$Y_{2,3} = \pm\sqrt{\frac{-\lambda\gamma_7}{\gamma_5\gamma_6}\left(T_f + \gamma_5^2\right)\left[\frac{\gamma_7}{\gamma_5\gamma_6}\left(T_f + \gamma_5^2\right) - \epsilon R_f\right]}, \tag{59}$$

$$Z_{2,3} = \epsilon R_f - \frac{\gamma_7}{\gamma_5\gamma_6}\left(T_f + \gamma_5^2\right),$$

$$V_{2,3} = 0,$$

are the convection solutions. The linear stability of the points can be obtained by linearizing the nonlinear dynamical system equation (55). Thus, the resulting Jacobian matrix is as follows:

$$M = \begin{pmatrix} 0 & 0 & 0 & 1 \\ \varepsilon r_f - Z & -\gamma_7 & -U & 0 \\ Y & U & -\lambda Pr_f & 0 \\ Pr_f\left[\gamma_6 \varepsilon r_f - Pr_f\left(T_f + \gamma_5^2\right)\right] & \gamma_6 Pr_f\left(\gamma_5 Pr_f - \gamma_7\right) & -\gamma_6 Pr_f U & 2\gamma_5 Pr_f \end{pmatrix}. \tag{60}$$

Using test solutions of the form $\exp\left(\xi t\right)$, $\xi \in \mathbb{C}$, the stability of the fixed point corresponding to the conduction solution is controlled by the roots of the following characteristic polynomial equation:

$$\left(\lambda\gamma_7 + \xi\right)\left\{\xi^3 + \left(2\gamma_5 Pr_f + \gamma_7\right)\xi^2 + \left[Pr_f^2\left(T_f + \gamma_5^2\right) + Pr_f\left(2\gamma_5\gamma_7 - \gamma_6 \epsilon R_f\right)\right]\xi^2 + Pr_f^2\left[\left(T_f + \gamma_5^2\right) - \gamma_5\gamma_6 \epsilon R_f\right]\right\} = 0. \tag{61}$$

This equation (61) generates four eigenvalues. The first one given by $\xi = -\lambda\gamma_7$ is always negative, and the other three are the solutions of the following equation:

$$\xi^3 + \left(2\gamma_5 Pr_f + \gamma_7\right)\xi^2 + \left[Pr_f^2\left(T_f + \gamma_5^2\right) + Pr_f\left(2\gamma_5\gamma_7 - \gamma_6 \epsilon R_f\right)\right]\xi + Pr_f^2\left[\gamma_7\left(T_f + \gamma_5^2\right) - \gamma_5\gamma_6 \epsilon R_f\right] = 0. \tag{62}$$

From this equation, the fixed point of the stationary solution is stable if and only if $\gamma_5\gamma_6 \epsilon R_f < \gamma_7\left(T_f + \gamma_5^2\right)$. Thus, the critical value of the rescaled Rayleigh number of the base fluid at which the fixed point of the stationary solution loses its stability and that of the convection solution takes over is expressed by

$$R_{fc1} = \frac{\gamma_7}{\epsilon\gamma_5\gamma_6}\left(T_f + \gamma_5^2\right). \tag{63}$$

This expression is a function of the thermophysical properties of the hybrid nanofluid and the rescaled Taylor number, so the transition from conduction to stationary convection depends on the volume fraction of the nanoparticles and the effect of rotation as shown in Figure 2.

Data analysis of the curves constructed in Figure 2 shows that when the value of Taylor number is less than about 0.33, 0.315, 0.30, and 0.293 for $\varphi_1 = \varphi_2 = 0.01, 0.02, 0.03$, and 0.04, respectively, R_{fc1} decreases but increases for higher values of T_f. Taking $T_f = 0$ for example, we found $R_{fc1} = 1.2$ like Gupta [10] for the ordinary fluids ($\varphi = 0$). But when $\varphi_1 = \varphi_2 = 0.01, 0.02, 0.03, 0.04$; we have $R_{fc1} \approx 1.176, 1.157, 1.142, 1.13$. Thus, it is then possible to reduce or increase conduction in a heat transfer fluid using hybrid nanoparticles under the effect of rotation. Using the same test solutions of the form $\exp\left(\xi t\right)$, $\xi \in \mathbb{C}$, the stability of the fixed points corresponding to the convection solution is controlled by the roots of the following characteristic polynomial equation:

$$\xi^4 + \left[\gamma_7\left(1 + \lambda\right) + 2\gamma_5 Pr_f\right]\xi^3 + \left[\frac{\lambda\gamma_5\gamma_6\gamma_7 \varepsilon R_f}{\left(T_f + \gamma_5^2\right)} + 2\gamma_5\gamma_7 Pr_f\left(1 + \lambda\right) + Pr_f\left(Pr_f - \frac{\gamma_7}{\gamma_5}\right)\left(T_f + \gamma_5^2\right)\right]\xi^2$$

$$+ \left\{\frac{2\lambda\gamma_5^2\gamma_6\gamma_7 \varepsilon R_f}{\left(T_f + \gamma_5^2\right)} + \lambda\gamma_7 Pr_f\left[\left(Pr_f - \frac{2\gamma_7}{\gamma_5}\right)\left(T_f + \gamma_5^2\right) + \gamma_6 \varepsilon R_f\right]\right\}\xi = 0. \tag{64}$$

This equation is solved numerically for different values of the parameters to study the stability of the fixed points of the convection solutions.

4.3.2. The Case of $\mathbf{C_f} \neq 0$. In the presence of the thermal relaxation time, the elimination of a quadratic factor, which is not associated with the beginning of the instability,
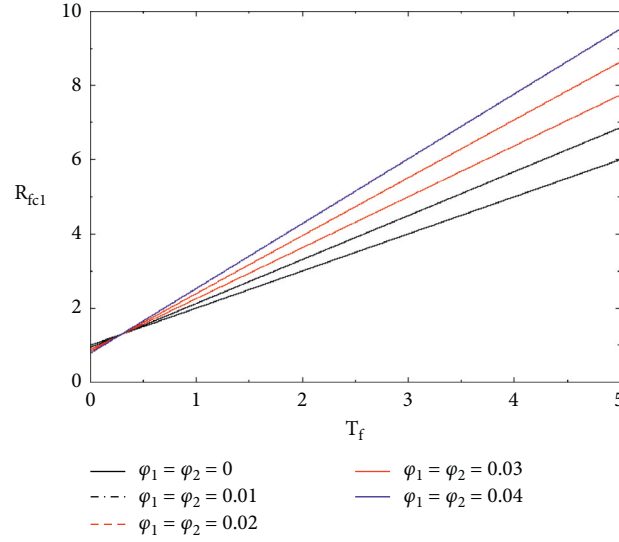
FIGURE 2: Variation of the critical Rayleigh number of the stationary solution as a function of the Taylor number with increasing nanoparticle volume fraction.

allowed us to find the characteristic polynomial equation of the fixed point corresponding to the immobile support at the origin whose roots control its stability, which is presented as follows:

$$
\begin{aligned}
& \xi^4 + \left(2\gamma_5 Pr_f + \delta\right)\xi^3 + \left\{\delta\left(2\gamma_5 Pr_f + \delta\right) - Pr_f\left[\gamma_6\epsilon R_f - Pr_f\left(T_f + \gamma_5^2\right)\right]\right\} \\
& \xi^2 + \left\{2\gamma_5\gamma_7\delta Pr_f - \gamma_6 Pr_f\left(2\gamma_5 Pr_f - \gamma_7\right)\epsilon R_f - \delta Pr_f\left[\gamma_6\epsilon R_f - Pr_f\left(T_f + \gamma_5^2\right)\right]\right\} \\
& + \delta Pr_f^2\left[\gamma_7\left(T_f + \gamma_5^2\right) - \gamma_5\gamma_6\epsilon R_f\right] = 0.
\end{aligned}
\tag{65}
$$

When $\xi = 0$, a stability exchange occurs and stationary convection takes over. The corresponding critical rescaled Rayleigh number of the base fluid from which this phenomenon is observed is equivalent to equation (63).

5. Results and Discussion

We performed numerical simulations to investigate the influence of hybrid nanoparticles and rotation on the dynamic behavior of thermal convection in a base fluid (water) in the presence of thermal relaxation time. Using free boundary conditions, we determined the analytical expressions of Rayleigh numbers of the base fluid for stationary and oscillatory convection as a function of the thermophysical properties of the hybrid nanofluid. We observe that the stationary Rayleigh number of the base fluid does not depend on the Prandtl number and the Cattaneo number. Figure 3 shows the variation of the stationary Rayleigh number of the base fluid as a function of wavelength for different values of the volume fraction of the hybrid nanoparticles (alumina-copper) with a fixed value of Taylor number. From these plotted curves, we find that the stationary Rayleigh number increases with the value of the volume fraction of hybrid nanoparticles. Thus, the addition of the hybrid nanoparticles (alumina-copper) to the base fluid (water) subjected to the rotation stabilizes the

stationary convection. Figure 4 shows the variation of the stationary Rayleigh number of the base fluid as a function of the wavelength for different values of the Taylor number with a fixed value of the volume fraction of the hybrid nanoparticles (alumina-copper).

From these plotted curves, it can be seen that the stationary Rayleigh number increases with an increasing Taylor number. Thus, the rotation stabilizes the stationary convection in the hybrid nanofluid.

The fourth-order Runge–Kutta method, the polynomial companion matrix, and the standard eigenvalue solver of the Lapack method are used to numerically solve systems equations (54) and (55). We took the initial conditions $U(0) = Y(0) = 0.8, Z(0) = 0.92195, P(0) = 0.8, S(0) = 0.92195$ and $V(0) = 0.8$. In order to guarantee the results, our different numerical simulations are compared with the results obtained by Dèdèwanou et al. [42] and Gupta [10]. We present in Figures 5–8, the bifurcation diagrams representing the minima and maxima of the posttransient regimes of the solutions of the amplitude $Z(t)$ as a function of function of R_f when the thermal relaxation time is zero using $Pr_f = 10$ and $\lambda = 8/3$. These diagrams show that system equation (55) can have chaotic, periodic, or multiperiodic behavior depending on the parameter values chosen. By comparing the diagrams in Figures 5–7, we notice that, for $T_f = 0.2$, when the volume fraction of the hybrid nanoparticles increases, the
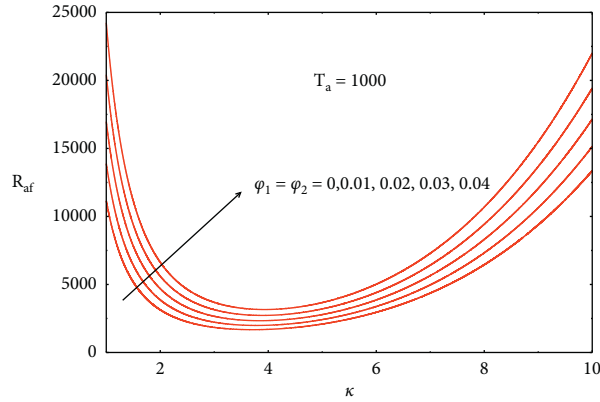
FIGURE 3: Variation of the stationary Rayleigh number of the base fluid as a function of the volume fraction of hybrid (aluminum-copper) nanoparticles.
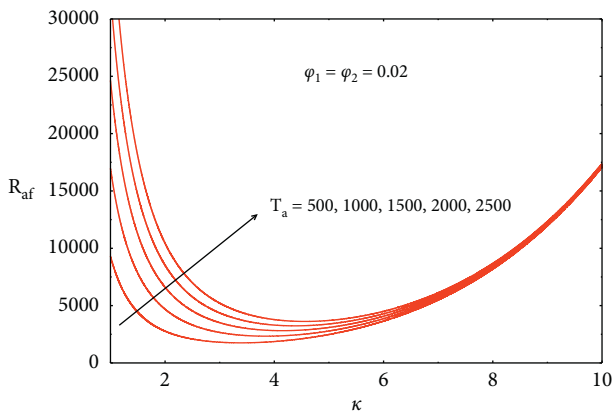

FIGURE 4: Variation of the stationary Rayleigh number of the base fluid as a function of the Taylor number.
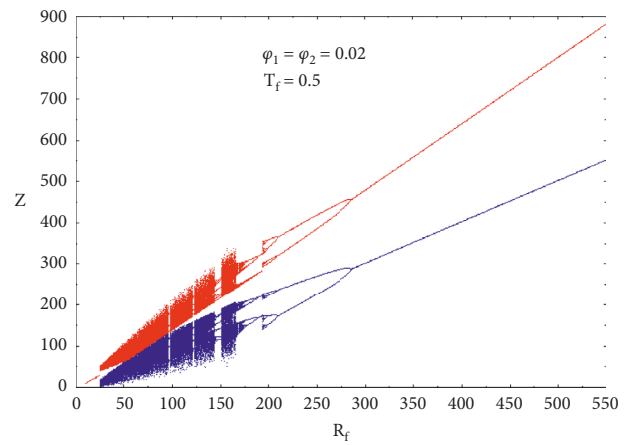

FIGURE 6: Bifurcation diagram of Z versus R_f representing maxima and minima of the posttransient solution of $Z(t)$ for hybrid nanofluid $\varphi_1 = \varphi_2 = 0.02$) with $T_f = 0.5$.
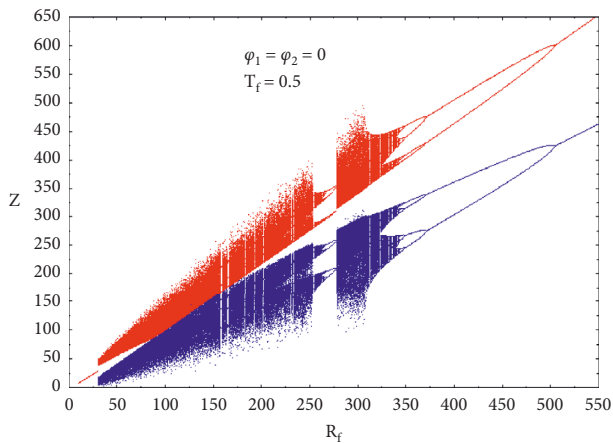

FIGURE 5: Bifurcation diagram of Z versus R_f representing maxima and minima of the posttransient solution of $Z(t)$ for hybrid nanofluid $\varphi_1 = \varphi_2 = 0$) with $T_f = 0.2$.
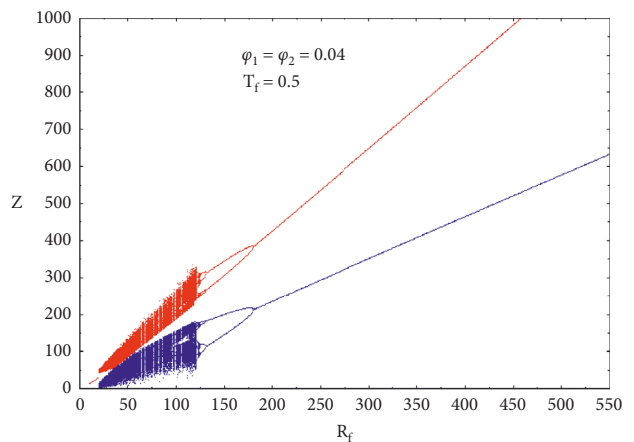

FIGURE 7: Bifurcation diagram of Z versus R_f representing maxima and minima of the posttransient solution of $Z(t)$ for hybrid nanofluid $\varphi_1 = \varphi_2 = 0.04$) with $T_f = 0.5$.

domain of the chaotic behavior chaotic behavior decreases with the increase of the values of the rescaled Rayleigh number of the number of the base fluid. On the other hand, comparison of the plots in Figures 6 and 8 shows that, for $\varphi_1 = \varphi_2 = 0.02$, increasing the values of the Taylor number increases the domain of chaotic behavior with increasing values of the rescaled Rayleigh number of the base fluid.
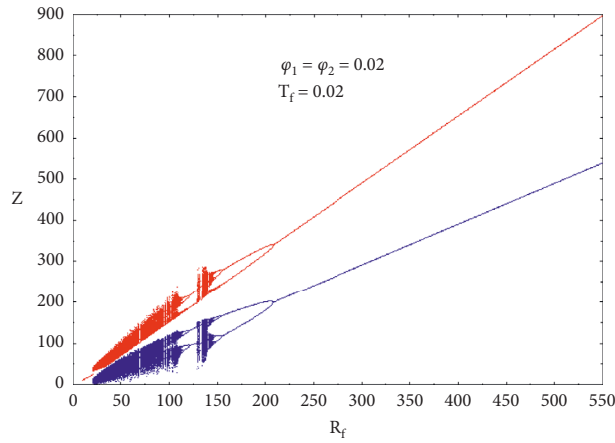
Figure 8: Bifurcation diagram of Z versus R_f representing maxima and minima of the posttransient solution of $Z(t)$ for hybrid nanofluid $\varphi_1 = \varphi_2 = 0.02$) with $T_f = 0.2$.
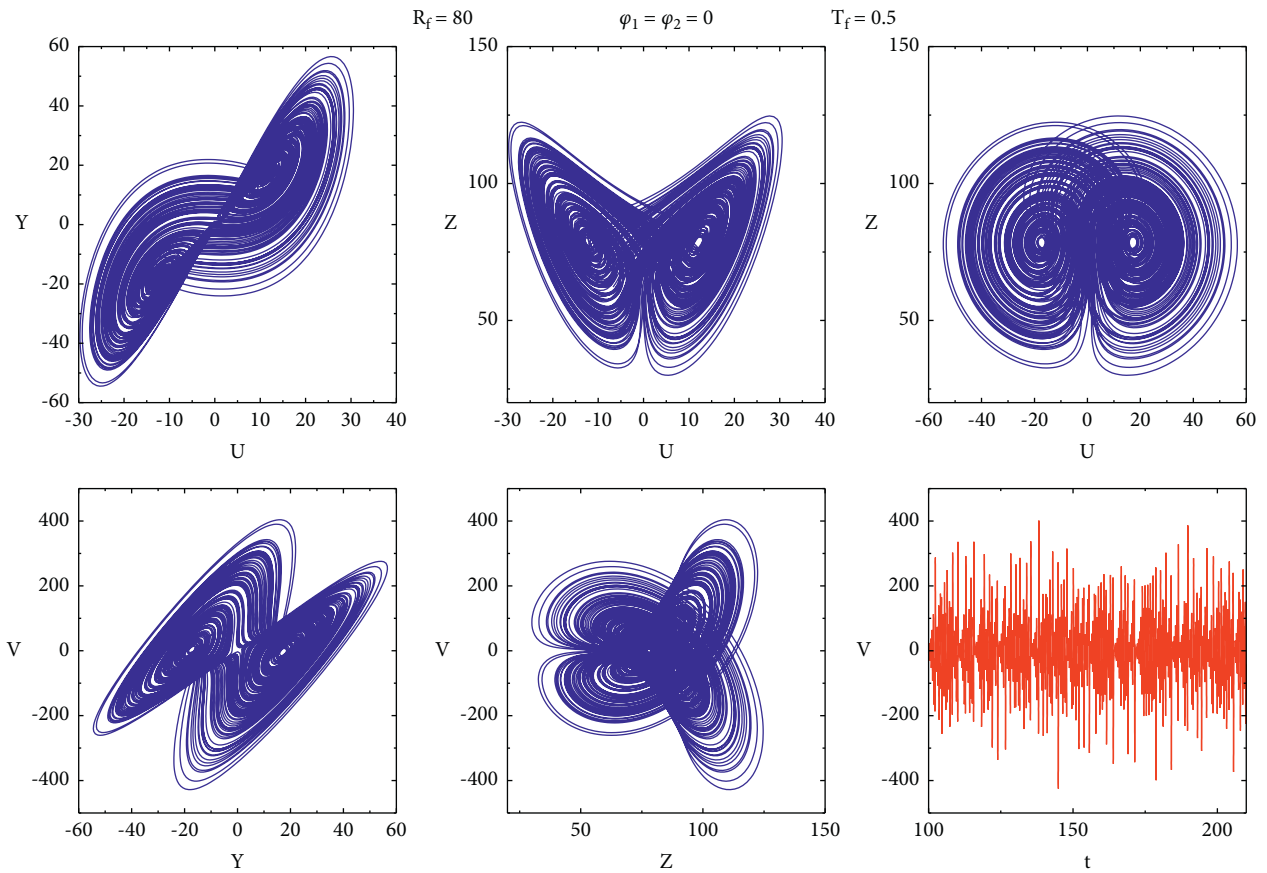

Figure 9: Phase portrait and its corresponding time story for $\varphi_1 = \varphi_2 = 0$), $R_f = 80$ and $T_f = 0.5$.

To confirm this prediction of the bifurcation diagrams, we constructed in Figure 9, the chaotic behavior of the system in the base fluid case by choosing $R_f = 80$ and $T_f = 0.5$. As shown in Figure 10, we set the values of the rescaled Taylor and Rayleigh numbers by varying the volume fraction of the hybrid nanoparticles to construct the in-plane
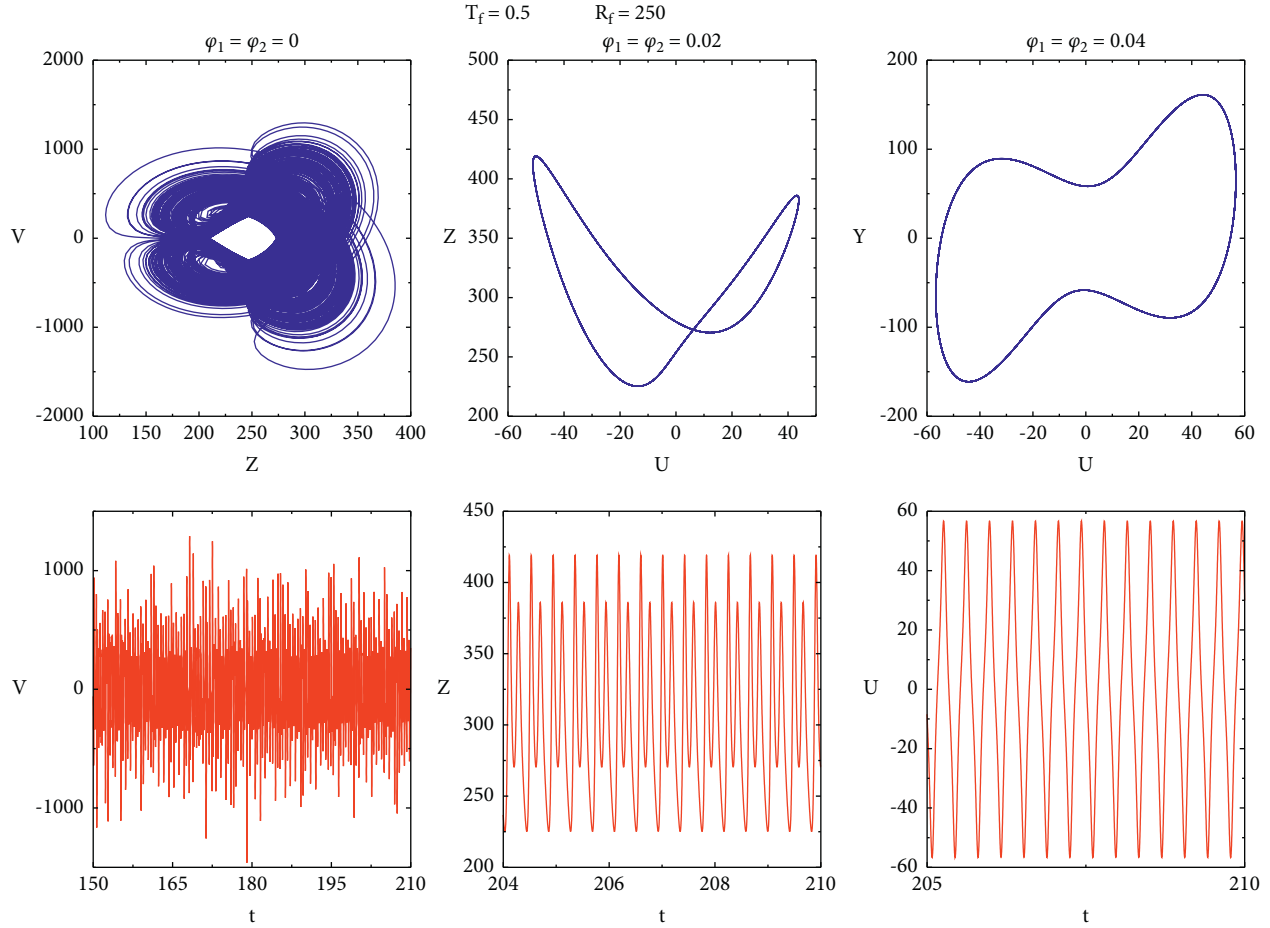
FIGURE 10: Phase portrait and its corresponding time story for $R_f = 250$, $T_f = 0.5$ and $\varphi_1 = \varphi_2 = 0, 0.02, 0.04$.

phase spaces with their corresponding time evolutions. For $\varphi_1 = \varphi_2 = 0, 0.02$ and 0.04, the system is chaotic in period 2 and period 1, respectively. Therefore, by analyzing these curves shown in Figure 10, it can be deduced that the addition of the hybrid nanoparticles in a heat transfer fluid makes the convection periodic. On the other hand, in the case of Figure 11, we have fixed the values of the volume fraction of hybrid nanoparticles and the rescaled Rayleigh number of the base fluid by varying the value of the rescaled Taylor number. The analysis of these curves shows that the system leaves the chaotic regime to the periodic regime when the value of the rescaled Taylor number decreases. Therefore, increasing the rescaled Taylor number increases the periodicity of the system.

Furthermore , we present in Figures 12–15, the bifurcation diagrams representing the minima and maxima of the post-transient regimes of the solutions of the amplitude $Z(t)$ as a function of R_f when the thermal relaxation time exists using $Pr_f = 5$ like Layek and Pati [41]. These diagrams show that system 63 can also have chaotic, periodic, or multiperiodic behavior depending on the parameter values chosen. Comparing the diagrams in Figures 12–14, it can be seen that, for

$T_f = 0.2$ and $C_f = 0.001$, increasing the volume fraction of the nanoparticles hybrid nanoparticles decreases the domain of chaotic behavior with the increase of the Rayleigh number values of the base fluid. On the other hand, the comparison of the diagrams in Figures 13 and 15 show that, for $\varphi_1 = \varphi_2 = 0.02$ and $T_f = 0.2$, increasing the values of the Cattaneo number largely increases the range of chaotic behavior with increasing values of the Rayleigh number of the base fluid. Referring to Figure 14, for $\varphi_1 = \varphi_2 = 0.04$, $T_f = 0.2$ and $C_f = 0.001$, the system is chaotic for $14 < R_f < 16$.

In Figures 16 and 17, we have constructed the phase spaces in the $X - Z$ plane for different values of the control parameters of system equation (54). When we set $T_f = 0.2$ and $C_f = 0.001$ (see Figure 16), we notice in the base fluid case ($\varphi_1 = \varphi_2 = 0$) that the system is in period 4 for $R_f = 166$. For $\varphi_1 = \varphi_2 = 0.02$, the system is in period 2 and for $\varphi_1 = \varphi_2 = 0.04$, the system has quasi-chaotic behavior. For $\varphi_1 = \varphi_2 = 0.02$ and $R_f = 100$ fixed, the system is in period 1 for $T_f = 0.2$ and $C_f = 0.001$. On the other hand, for $T_f = 0.2$ and $C_f = 0.003$, $T_f = 0.2$ and $C_f = 0.005$, $T_f = 0.3$ and $C_f = 0.005$, $T_f = 0.5$ and $C_f = 0.001$, and $T_f = 1.7$ and $C_f = 0.005$, the system is chaotic.
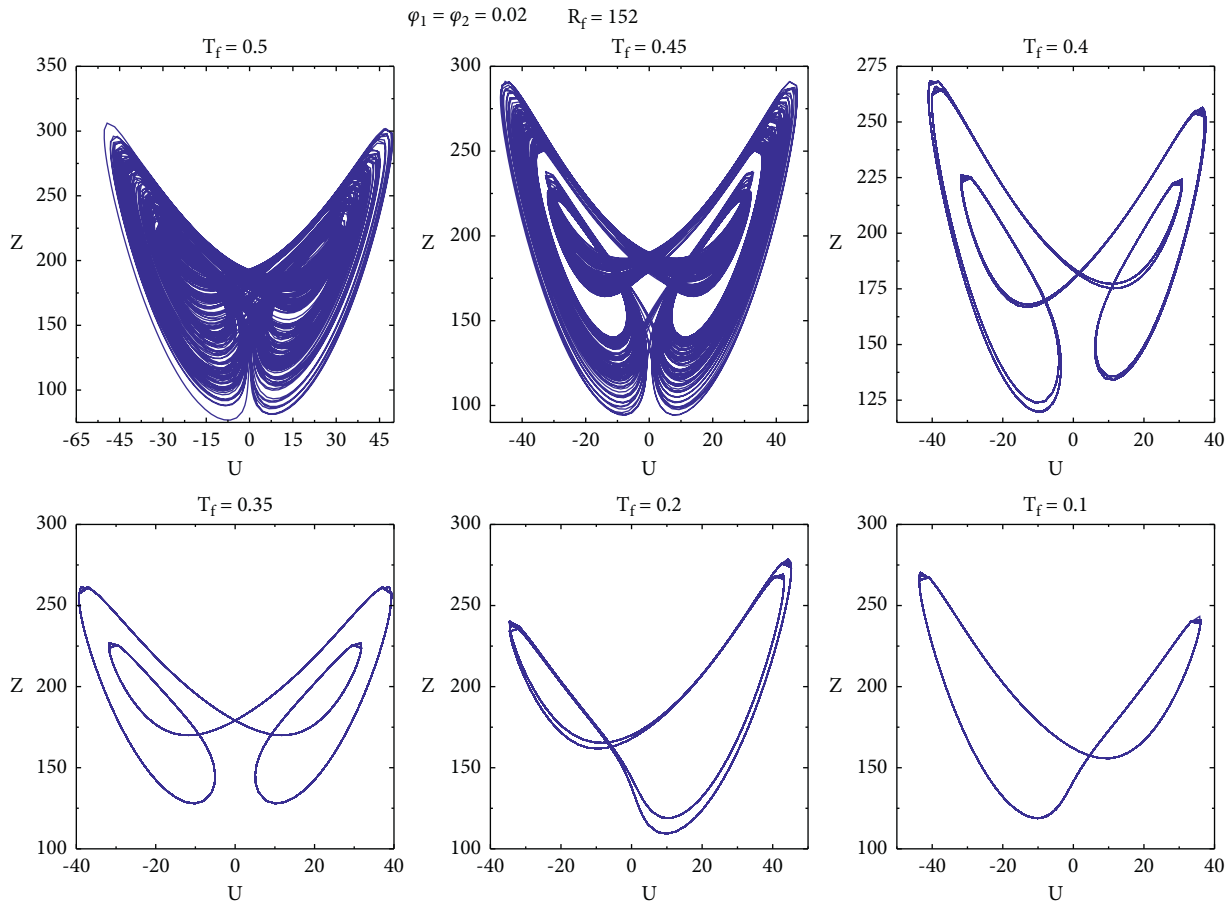
$\varphi_1 = \varphi_2 = 0.02$ $R_f = 152$

Figure 11: Phase portrait for $R_f = 152$ and $\varphi_1 = \varphi_2 = 0.02$ with different values of T_f.
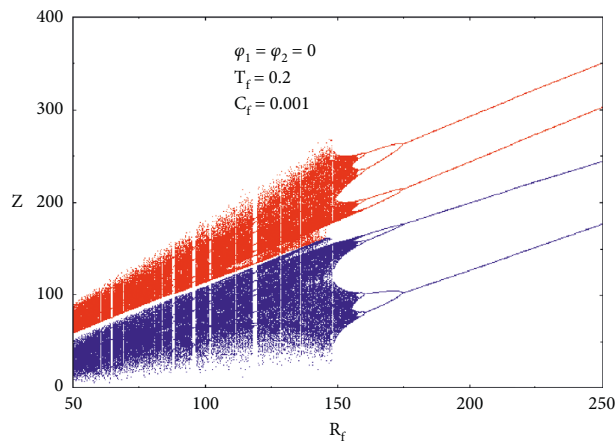

Figure 12: Bifurcation diagram of Z versus R_f representing maxima and minima of the posttransient solution of $Z(t)$ for base fluid ($\varphi_1 = \varphi_2 = 0$) with $T_f = 0.2$ and $C_f = 0.001$.
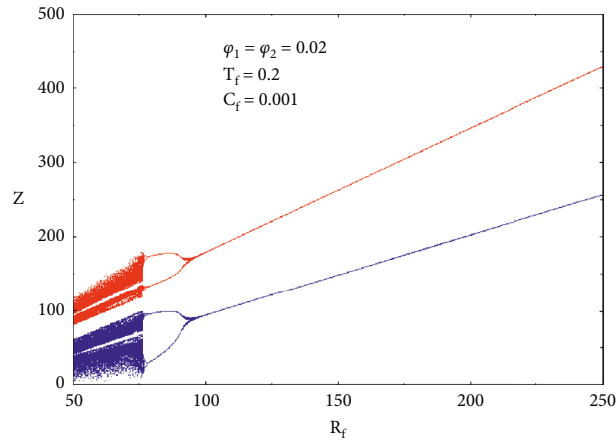
FIGURE 13: Bifurcation diagram of Z versus R_f representing maxima and minima of the posttransient solution of $Z(t)$ for hybrid nanofluid ($\varphi_1 = \varphi_2 = 0.02$) with $T_f = 0.2$ and $C_f = 0.001$.

FIGURE 14: Bifurcation diagram of Z versus R_f representing maxima and minima of the posttransient solution of $Z(t)$ for hybrid nanofluid ($\varphi_1 = \varphi_2 = 0.04$) with $T_f = 0.2$ and $C_f = 0.001$.

FIGURE 15: Bifurcation diagram of Z versus R_f representing maxima and minima of the posttransient solution of $Z(t)$ for hybrid nanofluid ($\varphi_1 = \varphi_2 = 0.02$) with $T_f = 0.2$ and $C_f = 0.005$.
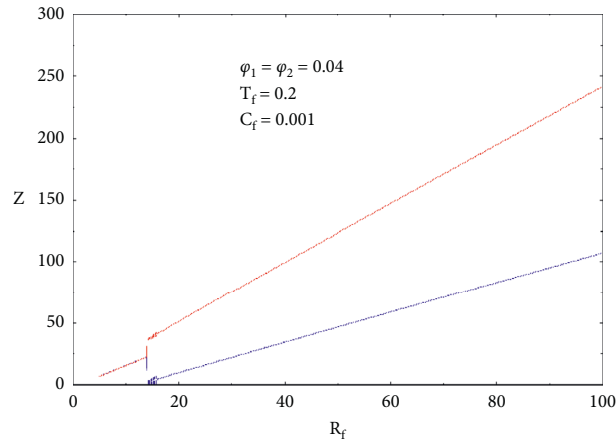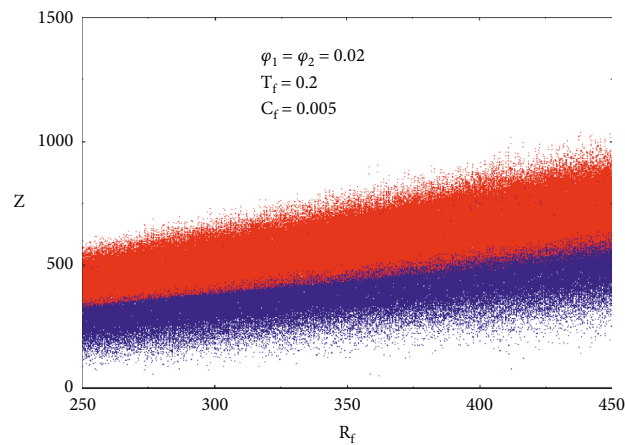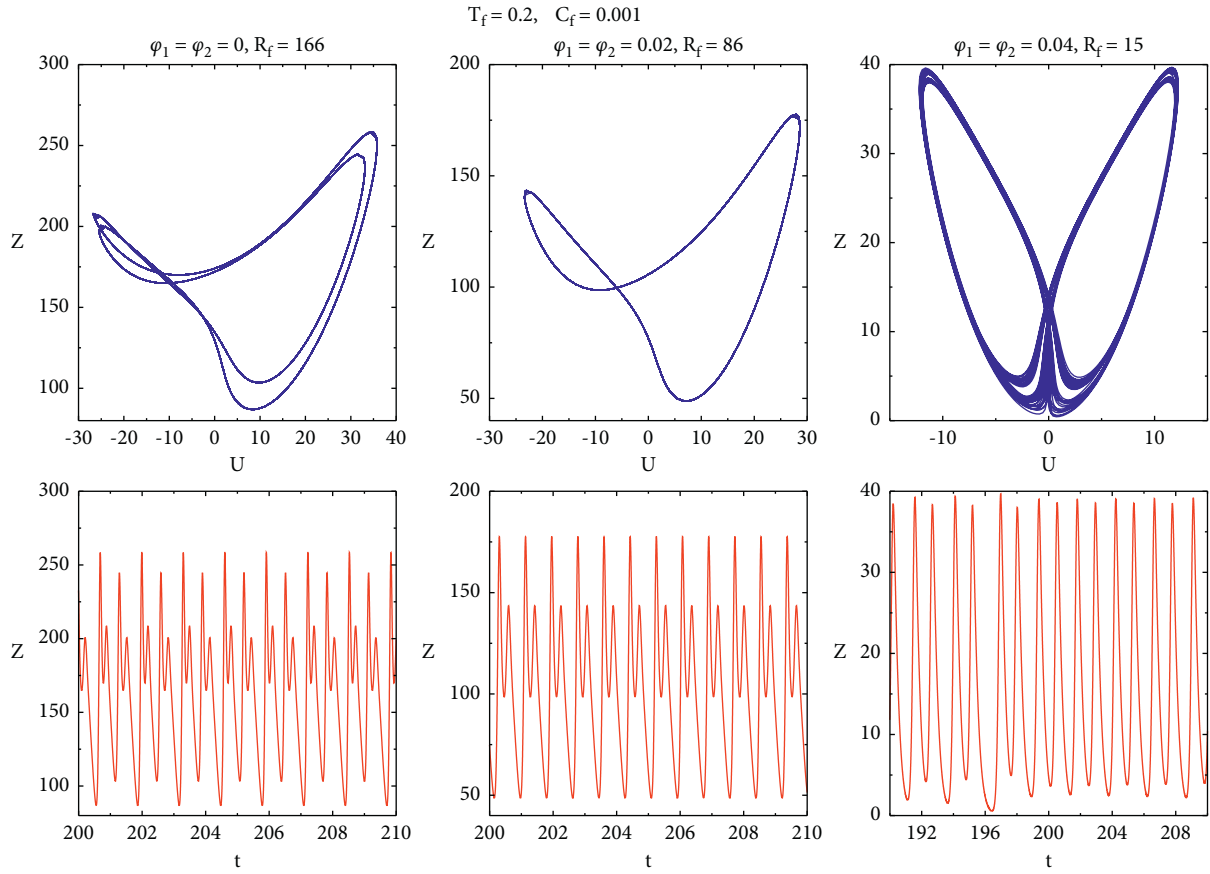
FIGURE 16: Phase portrait and its corresponding time story for $T_f = 0.2$ and $C_f = 0.001$.
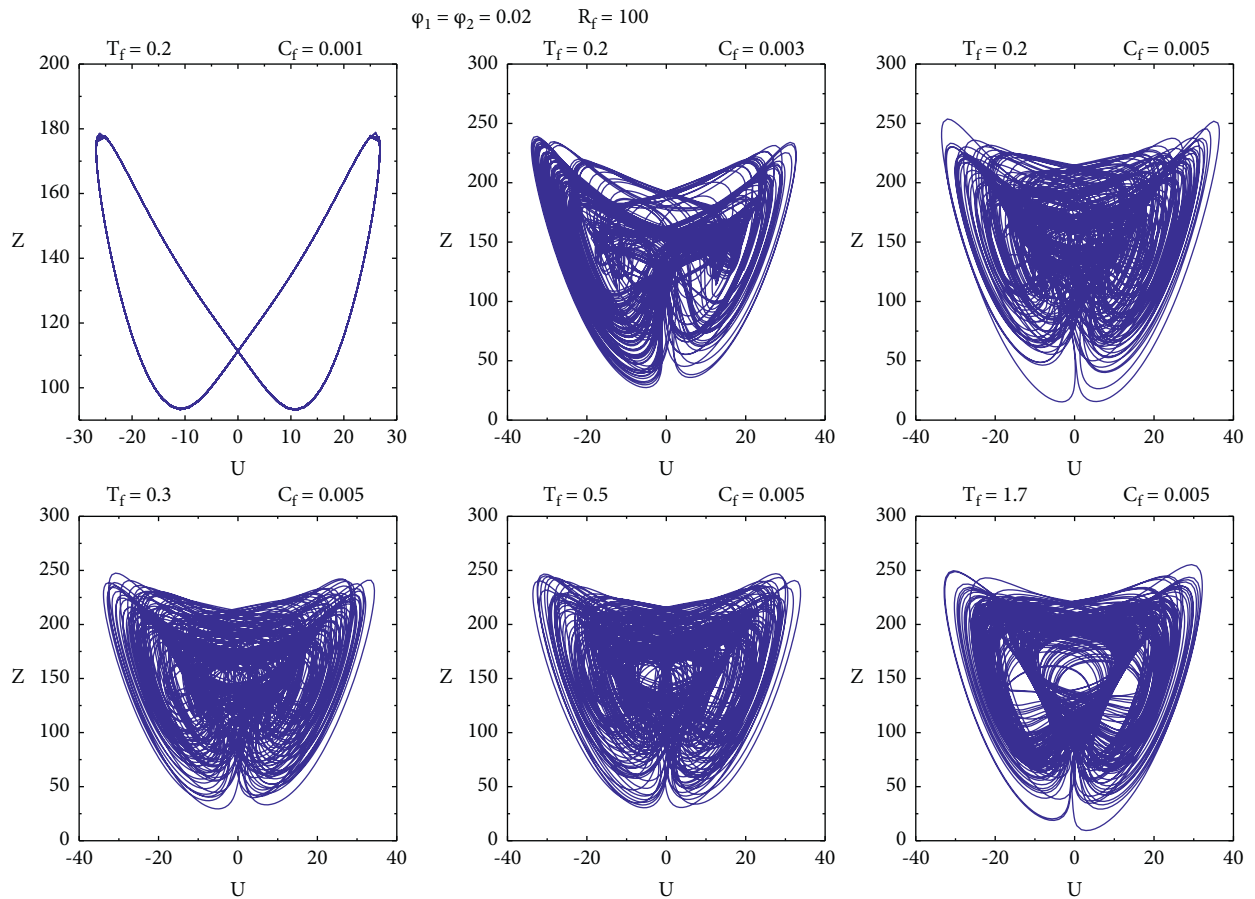

FIGURE 17: Phase portrait and its corresponding time story for $\varphi_1 = \varphi_2 = 0.02$ and $R_f = 100$.

6. Conclusions

We have studied the occurrence of thermal convective instabilities and chaos in a rotating infinite horizontal hybrid nanofluid layer heated from below with the Cattaneo–Christov heat flux model and subjected to unconstrained boundary conditions. The linear study of the mass, momentum, energy, and heat flow equations governing natural convection allowed us to find the general expression for the stationary Rayleigh number of the base fluid that can be used for the nonlinear dynamic analysis of thermal convection in nanofluids. We noticed that the rotation and the addition of nanoparticles in the base fluid have stabilizing effects on the stationary convection. With the obtained low-dimensional dynamical systems, we notice that the addition of hybrid nanoparticles in the heat transfer fluid subjected to rotation and/or in the presence of the thermal relaxation time reduces the domain of chaos and enlarges the domain of periodicity with the increase of the Rayleigh number of the base fluid. On the other hand, the increase of the Taylor number and Cattaneo number increases the chaotic domain with the increase of the Rayleigh number of the base fluid. The obtained nonlinear system depends on the parameters of the base fluid and the thermophysical properties of the hybrid nanofluid; it will be very useful to predict or control the chaotic behaviour of thermal convection in dynamic and biological systems. Thus, the hybrid nanofluid confers a great advantage for chaos control in many industrial applications like food processing, chemical processes, solidification and centrifugal casting of metals, and rotating machines to achieve the desired results. Obtained results and comparative studies show that the use of hybrid nanoparticles can be useful to control the small thermal relaxation time due to thermal inertia for thermal transport in biological tissues and surgical operations.

Latin symbols

A_{11}:	Stream function amplitude
B_{11}, B_{02}:	Temperature amplitude
C:	Cattaneo number
Cp:	Specific heat at constant pressure (J.kg^{-1}: K^{-1})
d/dt:	Material derivative
$\overrightarrow{e}_n$:	Unit vector normal to the boundary
$h(x; y)$:	Plane tiling function
$\overrightarrow{g}$, g:	Acceleration vector of gravity, gravity intensity (m.s^{-2})
k:	Thermal conductivity (W.m^{-1}.K^{-1})
m:	Particle shape factor
M:	Matrix associated to the origin fixed point
P:	Pressure (Pa)
Pr:	Prandtl number
Q:	Heat flux
Ra:	Thermal Rayleigh number
R_f:	Rescaled Rayleigh number of the base fluid
t:	Time (s)
Ta:	Taylor number
T_f:	Rescaled Taylor number

T_c:	Hot temperature (K)
T_0:	Cold temperature (K)
T:	Temperature at time t (K)
$U; Y; Z; P; S; V$:	Rescaled amplitudes
$\overrightarrow{v}$:	velocity vector
W:	Velocity eigenfunction
(x, y, z):	Cartesian coordinates

Greek symbols

α:	Thermal diffusivity of the fluid (m^{-2}.s^{-1})
β:	Coefficient of thermal expansion (K^{-1})
γ_i:	Nanofluid parameters
δ:	Rescaled Cattaneo number
ϵ:	Parameter related to nanofluid properties
ζ:	Vorticity
ϑ:	Volume
κ:	Wavenumber
μ:	Dynamic viscosity (kg.m^{-1}.s^{-1})
ξ:	Eigenvalues
ρ:	Density (kg.m^{-3})
τ:	Thermal relaxation time
φ_1:	Alumina volume fraction
φ_2:	Copper volume fraction
χ:	Temperature gradian
ω:	Oscillatory frequency
Θ:	Temperature eigenfunction
Φ:	Heat-flux eigenfunction
ψ:	Stream function
Ω:	Angular velocity

Subscripts

$*$:	Dimensionless
$\sim$:	Small quantity
b:	Basic solution
c:	Critical
f:	Base fluid
hf:	Hybrid nanofluid
s:	Nanoparticle
0:	Reference.

Data Availability

No data were used to support this study.

Conflicts of Interest

The authors declare that they have no conflicts of interest.

Acknowledgments

References

[1] S. U. S. Choi and J. A. Eastman, "Enhancing thermal conductivity of fluids with nanoparticles," in *Proceedings of the 1995 International Machanical Engineering Congress and*

Exposition, vol. 66, no. 4356, pp. 99–105, ASME, San Francisco, NY, USA, November 1995.

[2] H. F. Oztop and E. Abu-Nada, "Numerical study of natural convection in partially heated rectangular enclosures filled with nanofluids," *International Journal of Heat and Fluid Flow*, vol. 29, no. 5, pp. 1326–1336, 2008.

[3] E. Abu-Nada, Z. Masoud, and A. Hijazi, "Natural convection heat transfer enhancement in horizontal concentric annuli using nanofluids," *International Communications in Heat and Mass Transfer*, vol. 35, no. 5, pp. 657–665, 2008.

[4] M. K. Das and P. Shridhar Ohal, "Natural convection heat transfer augmentation in a partially heated and partially cooled square cavity utilizing nanofluids," *International Journal of Numerical Methods for Heat and Fluid Flow*, vol. 19, no. 3/4, pp. 411–431, 2009.

[5] K. C. Lin and A. Violi, "Natural convection heat transfer of nanofluids in a vertical cavity: effects of non-uniform particle diameter and temperature on thermal conductivity," *International Journal of Heat and Fluid Flow*, vol. 31, no. 2, pp. 236–245, 2010.

[6] B. Elhajjar, G. Bachir, A. Fakih, and C. Charrier-Mojtabi, "Modeling of Rayleigh-Bénard natural convection heat transfer in nanofluids," *Comptes Rendus Mecanique*, vol. 338, no. 6, pp. 350–354, 2010.

[7] B. Mahanthesh, "Flow and heat transport of nanomaterial with quadratic radiative heat flux and aggregation kinematics of nanoparticles," *International Communications in Heat and Mass Transfer*, vol. 127, Article ID 105521, 2021.

[8] G. Shalini and B. Mahanthesh, "Rayleigh-benard convection in a dusty Newtonian nanofluid with and without Coriolis force," *Journal of Nanofluids*, vol. 7, no. 6, pp. 1240–1246, 2018.

[9] J. Ahuja and J. Sharma, "Rayleigh-Bénard instability in nanofluids: a comprehensive review," *Micro and Nano Systems Letters*, vol. 8, no. 1, p. 15, 2020.

[10] V. K. Gupta, B. S. Bhadauria, I. Jawdat, J. Singh, and A. Singh, "Chaotic convection in a rotating fluid layer," *Alexandria Engineering Journal*, vol. 54, no. 4, pp. 981–992, 2015.

[11] A. Jan, B. Mir, and A. A. Mir, "Hybrid nanofluids: an overview of their synthesis and thermophysical properties," in *Proceedings of the Tech. Conf. And Exhibition on Integration and Packaging of MEMS, NEMS, and Electronic System*, pp. 343–353, 2019.

[12] A. M. Rashad, A. J. Chamkha, and M. A. Ismael, "MHD natural convection in a triangular cavity filled with a Cu-Al_2O_3/water hybrid nanofluid with localized heating from below and internal heat generation," *Journal of Heat Transfer*, vol. 140, no. 7, Article ID 072502, 13 pages, 2018.

[13] N. A. L. Aladin, N. Bachok, and I. Pop, "Water hybrid nanofluid flow over a permeable moving surface in presence of hydromagnetic and suction effects," *Alexandria Engineering Journal*, vol. 59, no. 2, pp. 657–666, 2020.

[14] S. Myson and B. Mahanthesh, "Rayleigh-bénard convection in Casson and hybrid nanofluids: an analytical investigation," *Journal of Nanofluids*, vol. 8, no. 1, pp. 222–229, 2019.

[15] J. Mackolil and B. Mahanthesh, "Optimization of heat transfer in the thermal Marangoni convective flow of a hybrid nanomaterial with sensitivity analysis," *Applied Mathematics and Mechanics*, vol. 42, no. 11, pp. 1663–1674, 2021.

[16] K. Thriveni, B. Mahanthesh, Sensitivity computation of nonlinear convective heat transfer in hybrid nanomaterial between two concentric cylinders with irregular heat sources," *International Communications in Heat and Mass Transfer*, vol. 129, Article ID 105677, 2021.

[17] J. M. Jawdat, I. Hashim, and S. Momani, "Dynamical system Analysis of thermal convection in a horizontal layer of nanofluids heated from below," *Mathematical Problems in Engineering*, vol. 2012, Article ID 128943, 13 pages, 2012.

[18] K. Moaddy, "Control and stability on chaotic convection in porous media with time delayed fractional orders," *Advances in Difference Equations*, vol. 2017, no. 1, 2017.

[19] K. Moaddy, A. Radwan, and J. Jawdat, "Bifurcation behaviour and control on chaotic convection of nanofluids with fractional-orders," *Recent Advances in Mathematical Methods and Computational Techniques in Modern Science*, pp. 63–72, 2013.

[20] R. Bhardwaj and M. Chawla, "Convection dynamics of nanofluids for temperature and magnetic field variations," *Advances in Intelligent Systems and Computing*, vol. 1165, pp. 271–289, 2020.

[21] S. J. Dèdèwanou, A. L. Hinvi, and H. C. Miwadinou, "Chaotic convection in a hyorizontal cavity filled with (alumina–copper)/water hybrid nanofluid Heated from below in Presence of Magnetic Field," *Brazilian Journal of Physics*, vol. 51, no. 4, pp. 1079–1095, 2021.

[22] C. I. Christov and P. M. Jordan, "Heat conduction paradox involving second-sound propagation in moving media," *Physical Review Letters*, vol. 94, no. 15, Article ID 154301, 2005.

[23] C. I. Christov, "On frame indifferent formulation of the Maxwell-Cattaneo model of finite-speed heat conduction," *Mechanics Research Communications*, vol. 36, no. 4, pp. 481–486, 2009.

[24] B. Straughan, "Thermal convection with the Cattaneo-Christov model," *International Journal of Heat and Mass Transfer*, vol. 53, no. 1-3, pp. 95–98, 2010.

[25] B. Mahanthesh, B. J. Gireesha, and C. S. K. Raju, "Cattaneo-Christov heat flux on UCM nanofluid flow across a melting surface with double stratification and exponential space dependent internal heat source," *Informatics in Medicine Unlocked*, vol. 9, pp. 26–34, 2017.

[26] J. Alebraheem and M. Ramzan, "Flow of nanofluid with Cattaneo-Christov heat flux model," *Applied Nanoscience*, vol. 10, no. 8, pp. 2989–2999, 2020.

[27] A. S. Dogonchi and D. D. Ganji, "Impact of Cattaneo-Christov heat flux on MHD nanofluid flow and heat transfer between parallel plates considering thermal radiation effect," *Journal of the Taiwan Institute of Chemical Engineers*, vol. 80, pp. 52–63, 2017.

[28] S. Jakeer, P. BalaAnki Reddy, A. M. Nabwey, and H. A. Nabwey, "Impact of heated obstacle position on magneto-hybrid nanofluid flow in a lid-driven porous cavity with Cattaneo-Christov heat flux pattern," *Alexandria Engineering Journal*, vol. 60, no. 1, pp. 821–835, 2021.

[29] A. Hafeez, M. Khan, A. Ahmed, and J. Ahmed, "Rotational flow of Oldroyd-B nanofluid subject to Cattaneo-Christov double diffusion theory," *Applied Mathematics and Mechanics*, vol. 41, no. 7, pp. 1083–1094, 2020.

[30] A. Ahmed, M. Khan, M. Ahmed, J. Iqbal, and Z. Iqbal, "Forced convection in 3D Maxwell nanofluid flow via Cattaneo-Christov theory with Joule heating," *Proceedings of the Institution of Mechanical Engineers - Part E: Journal of Process Mechanical Engineering*, vol. 235, no. 4, pp. 747–757, 2021.

[31] A. Saeed, S. Islam, A. Shah, Z. Kumam, P. Khan, and W. Khan, "Influence of cattaneo-christov heat flux on MHD jeffrey, Maxwell, and Oldroyd-B nanofluids with homogeneous-heterogeneous reaction," *Symmetry*, vol. 11, no. 3, p. 439, 2019.

[32] H. Gul, M. Ramzan, J. D. Chu, Y. M. Kadry, and S. Kadry, "Multiple slips impact in the MHD hybrid nanofluid flow with Cattaneo-Christov heat flux and autocatalytic chemical reaction," *Scientific Reports*, vol. 11, no. 1, Article ID 14625, 2021.

[33] D. Lu, M. Ramzan, M. Howari, F. Chung, and J. D. Chung, "A thin film flow of nanofluid comprising carbon nanotubes influenced by Cattaneo-Christov heat flux and entropy generation," *Coatings*, vol. 9, no. 5, p. 296, 2019.

[34] Y. Zhang, N. Shahmir, M. Alotaibi, H. Aljohani, and H. M. Aljohani, "Upshot of melting heat transfer in a Von Karman rotating flow of gold-silver/engine oil hybrid nanofluid with Cattaneo-Christov heat flux," *Case Studies in Thermal Engineering*, vol. 26, Article ID 101149, 2021.

[35] S. B. Yu-Ming Chu and M. Ramzan, "Model-based Comparative Study of Magnetohydrodynamics Unsteady Hybrid Nanofluid Flow between Two Infinite Parallel Plates with Particle Shape Effects," *Mathmatical Methods in applied Sciences*, Wiley Online Library, NJ, USA, 2022.

[36] M. Ramzan, H. Gul, M. Y. Baleanu, D. Nisar, and K. S. Nisar, "On hybrid nanofluid Yamada-Ota and Xue flow models in a rotating channel with modified Fourier law," *Scientific Reports*, vol. 11, no. 1, Article ID 19590, 2021.

[37] M. Ramdan, N. Shahmir, H. A. S. Nisar, K. S. Alharbi, F. M. Yahia, and I. S. Yahia, "Hydrodynamic and heat transfer analysis of dissimilar shaped nanoparticles-based hybrid nanofluids in a rotating frame with convective boundary condition," *Scientific Reports*, vol. 12, no. 1, 2022.

[38] N. Abid, M. Ramzan, J. D. Kadry, S. Chu, and Y. M. Chu, "Comparative analysis of magnetized partially ionized copper, copper oxide-water and kerosene oil nanofluid flow with Cattaneo-Christov heat flux," *Scientific Reports*, vol. 10, no. 1, p. 436, 2020.

[39] M. Ramzan, H. Gul, and S. Kadry, "Onset of Cattaneo-Christov heat flux and thermal stratification in ethylene-glycol based nanofluid flow containing carbon nanotubes in a rotating frame," *IEEE Access*, vol. 7, pp. 146190–146197, 2019.

[40] Y. M. Chu, M. Ramzan, N. Shaheen et al., "Analysis of Newtonian heating and higher-order chemical reaction on a Maxwell nanofluid in a rotating frame with gyrotactic microorganisms and variable heat source/sink," *Journal of King Saud University Science*, vol. 33, no. 8, Article ID 101645, 2021.

[41] G. C. Layek and N. C. Pati, "Bifurcations and chaos in convection taking non-Fourier heat-flux," *Physics Letters A*, vol. 381, no. 41, pp. 3568–3575, 2017.

[42] S. J. Dèdèwanou, A. V. Monwanou, A. A. Koukpémèdji, L. A. Hinvi, C. H. Miwadinou, and J. B Chabi Orou, "Thermal instability and chaos in a hybrid nanofluid flow," *International Journal of Bifurcation and Chaos*, vol. 32, no. 07, Article ID 2250102, 21 pages, 2022.

[43] J. J. Bissell, "On oscillatory convection with the Cattaneo-Christov hyperbolic heat-flow model," *Proceedings of the Royal Society A: Mathematical, Physical & Engineering Sciences*, vol. 471, no. 2175, Article ID 38527619, 2015.

[44] S. Chandrasekhar, *Hydrodynamic and Hydromagnetic Stability*, Dover, NY, USA, 1981.

[45] E. N. Lorenz, "Deterministic nonperiodic flow," *Journal of the Atmospheric Sciences*, vol. 20, no. 2, pp. 130–141, 1963.

[46] C. Sparrow, "The Lorenz Equations: Bifurcations, Chaos and Strange Attractors," *Applied Mathematical Sciences I*, vol. 41, 1982.